Elucidating the Functions of Protein Disulfide Isomerase Family Proteins during Quality Control in the Endoplasmic Reticulum

by

Michele L. Forster

A dissertation submitted in partial fulfillment
of the requirements for the degree of
Doctor of Philosophy
(Cell and Developmental Biology)
in the University of Michigan
2009

Doctoral Committee:

Associate Professor Billy Tsai, Chair
Professor Peter Arvan
Associate Professor Roland P. Kwok
Associate Professor Kristen J. Verhey

Acknowledgements

I am grateful to the following persons for their guidance, assistance, and support throughout this endeavor: my mentor Billy Tsai; members of my thesis committee Kristen J. Verhey, Peter Arvan, and Roland P. Kwok; my dear friends and outstanding colleagues Kaleena Bernardi Dezsi, Emily Rainey-Barger, and Cheryse Furman; departmental administrator Kristen Hug; computer support technician Ryan Schell; my family and friends who are like family, with special thanks to David.

I thank the following persons for generating data presented in this thesis: Kelsey Sivick (Figure 2.4 Part A, right panel), Billy Tsai (Figure 2.5), Young-nam Park (Figure 2.6 Part C), and James J. Mahn. (Figure 3.5 Part C).

Contents

Acknowledgements ii
List of Figures iv
Abstract v
Chapter
1. Introduction 1
2. Protein Disulfide Isomerase Family Proteins Play Opposing Roles during Quality Control in the Endoplasmic Reticulum 7
3. Generating an Unfoldase from Thioredoxin-like Domains 27
4. Conclusion 47
References 51

List of Figures

Figure

1.1 Crystal structure of cholera toxin 5
1.2 Intracellular trafficking of cholera toxin 5
1.3 The human protein disulfide isomerase family 6
2.1 Diagram of the domain compositions of PDI, ERp72, and ERp57 19
2.2 Retrotranslocation of CTA1 20
2.3 Down-regulation of PDI family proteins 21
2.4 PDI and ERp72 play opposing roles during CT retrotranslocation 22
2.5 PDI and ERp72 exert opposing effects on the conformation of CT 24
2.6 General roles for PDI and ERp72 during ER quality control 25
3.1 Recombinant PDI unfolds CTA1 efficiently 40
3.2 PDI's bb'xa' domains form the minimum unit required to unfold CTA1 41
3.3 A PDI-toxin interaction is necessary but not sufficient to trigger unfolding 42
3.4 The specific linear arrangement and identity of domains are determinants of unfoldase activity 43
3.5 Functional differences between thioredoxin-like domains of PDI and ERp57 44
3.6 Functional differences between thioredoxin-like domains of PDI and ERp72 46
4.1 PDI family proteins play opposing roles during ER quality control 50

Abstract

The quality control system in the endoplasmic reticulum (ER) retains newly synthesized proteins in the organelle until they are folded properly and mediates the ER-to-cytosol transport (*i.e.*, retrotranslocation) of misfolded proteins for proteasomal degradation. In mammalian cells, the A1 subunit of cholera toxin (CTA1) uses the retrotranslocation machinery to reach the cytosol where it induces toxicity. Using a semi-permeabilized cell system characterized here, we found the ER factor protein disulfide isomerase (PDI) facilitates CTA1 retrotranslocation consistent with its previously demonstrated ability to unfold the toxin *in vitro*. In contrast, the PDI family protein ERp72 retains CTA1 in the ER and stabilizes a folded conformation of the toxin. Furthermore, we show the opposing functions of PDI and ERp72 in retrotranslocation versus ER retention operate on endogenous proteins misfolded in the ER. Collectively, our data indicate that PDI family proteins play opposing roles during ER quality control and establish an assay to study CTA1 retrotranslocation.

Because PDI's ability to unfold CTA1 *in vitro* correlates with its ability to facilitate the toxin's retrotranslocation, we investigated the mechanism of this unfoldase activity. PDI comprises two redox-active (*a* and *a'*) and two redox-inactive (*b* and *b'*) thioredoxin-like domains, a linker (*x*), and a C-terminal domain (*c*) arranged *abb'xa'c*. Using recombinant PDI fragments, we show that binding of CTA1 by the continuous *bb'xa'* fragment is necessary and sufficient to trigger unfolding. The specific linear arrangement of *bb'xa'* and type of *a* domain (*a'* versus *a*) C-terminal to *bb'x* are additional determinants of activity. These data suggest a general mechanism for PDI's unfoldase activity: the concurrent and specific binding of *bb'xa'* to particular regions along the CTA1 molecule triggers its unfolding. Furthermore, we show PDI's *bb'* domains are indispensable to the unfolding reaction, whereas the function of its *a'* domain can be replaced partially by the *a'* domain from ERp57 (*abb'xa'c*) or ERp72 (*ca°abb'xa'*), PDI family proteins that do

not unfold CTA1 normally. However, PDI's *bb'* domains were insufficient to convert full-length ERp57 into an unfoldase because ERp57's *a* domain inhibited toxin binding. Thus, we propose that generating an unfoldase from thioredoxin-like domains requires PDI's *bb'(x)* domains followed by an *a'* domain but not preceded by an *a* domain that can interfere with binding.

Chapter 1

Introduction

Newly synthesized polypeptides destined for the secretory pathway fold in the endoplasmic reticulum (ER) with the help of ER chaperones, thiol oxidoreductases, and other enzymes (reviewed in Buck et al., 2007). Nevertheless, it is common for proteins to misfold (reviewed in Goldberg, 2003). To protect cells from potentially harmful effects of misfolded proteins (reviewed in Ni and Lee, 2007), ER residents form a quality control system that allows only correctly folded proteins to reach their intended destinations and disposes of misfolded proteins (reviewed in Ellgaard and Helenius, 2003). Accordingly, nascent polypeptides are retained in the ER until they are folded properly and terminally misfolded proteins are transported across the ER membrane into the cytosol (*i.e.*, retrotranslocated) for proteasomal degradation, a process called ER-associated degradation (ERAD). These mechanisms are exploited by several virulence factors to exert their pathogenic effects in mammalian cells (reviewed in Tsai et al., 2002). Because of its relevance to human health, it is important to understand the factors and mechanisms that govern ER quality control. Over the past decade, many components of this system have been identified; their precise functions and substrate specificities are current areas of investigation (reviewed in Nakatsukasa and Brodsky, 2008).

This thesis focuses on the role of mammalian protein disulfide isomerase (PDI) during ER quality control. PDI is abundantly expressed in the ER lumen of all eukaryotic cells (reviewed in Ferrari and Soling, 1999). It is primarily known as a catalyst of oxidative protein folding (Goldberger et al., 1964), but also functions as a chaperone, binding polypeptides to prevent their aggregation, independent of redox activity (Song and Wang, 1995; Wang and Tsou, 1993; Winter et al., 2002). In contrast to these activities, PDI has been implicated in retrotranslocation. For example, PDI was shown to associate with a

misfolded protein in the ER before its proteasomal degradation in the cytosol (Molinari et al., 2002). Furthermore, PDI was shown to unfold the catalytic A1 subunit of cholera toxin (CTA1; Tsai et al., 2001), a step presumably required for the toxin's retrotranslocation into the cytosol where it induces toxicity (Lencer and Tsai, 2003). We therefore hypothesized that PDI facilitates the retrotranslocation of both CTA1 and misfolded proteins destined for ERAD.

Cholera toxin (CT) is secreted by the bacterium *Vibrio cholerae* and intoxicates intestinal epithelial cells in mammals causing secretory diarrhea (reviewed in Lencer and Tsai, 2003). The holotoxin comprises a single A subunit (CTA) and a homopentameric B subunit (CTB) joined noncovalently (Fig 1.1; Zhang et al., 1995). Upon secretion from the bacterium, extracellular proteases cleave CTA into the A1 and A2 polypeptides (CTA1 and CTA2, respectively; Lencer et al., 1997), which are joined by a disulfide bond and noncovalent interactions (Mekalanos et al., 1979; Zhang et al., 1995). To intoxicate a cell, CTB binds the ganglioside GM1 on a cell's surface, and the holotoxin undergoes retrograde transport through the secretory pathway to the ER lumen (Fig. 1.2; Fujinaga et al., 2003). In the ER, the disulfide bond joining CTA1 and CTA2 is reduced (Majoul et al., 1996), and CTA1 is presumably unfolded by PDI and dissociates from the holotoxin (Tsai et al., 2001). Unfolded CTA1 then undergoes retrotranslocation to the cytosol through a protein channel that appears to include Derlin-1 (Bernardi et al., 2008), while CTB remains in the ER (Fujinaga et al., 2003). In the cytosol, CTA1 is resistant to ubiquitination and therefore avoids proteasomal degradation (Rodighiero et al., 2002). Instead, it refolds and ADP-ribosylates the heterotrimeric G protein Gαs, which constitutively activates adenylyl cyclase to produce cAMP (Sears and Kaper, 1996). This increase in intracellular cAMP triggers chloride secretion that results in diarrhea.

To test our hypothesis that PDI facilitates the retrotranslocation of CTA1 and proteins misfolded in the ER, we analyzed the effects of changing PDI's protein level in cells on the retrotranslocation of CTA1, a misfolded secretory protein (mutant thyroglobulin), and a general population of ERAD substrates (Chapter 2; Forster et al., 2006). We found that PDI facilitates the retrotranslocation of each substrate tested, indicating that it is a general

component of the retrotranslocation machinery. Furthermore, we identified structural features of PDI required to unfold CTA1, providing insight into the mechanism of this activity (Chapter 3; Forster, 2008).

In addition to PDI, we studied the functions of two PDI family proteins during ER quality control. PDI is the founding member of a family of approximately twenty proteins in mammals (Fig. 1.3; reviewed in Ellgaard and Ruddock, 2005). Each member contains at least one domain with structural homology to cytoplasmic thioredoxin and is localized to the ER. Their thioredoxin-like domains are either redox active (a-type) or redox inactive (b-type) (Kemmink et al., 1997). Many family members differ from each other in the number of a-type and b-type domains, their redox active sequences, and/or the presence of various other domains (reviewed in Appenzeller-Herzog and Ellgaard, 2008). However, two PDI family proteins, ERp57 and ERp72, closely resemble PDI in domain composition, expression pattern, and redox active sequences (reviewed in Maattanen et al., 2006).

Similar to PDI, ERp57 and ERp72 are catalysts of oxidative protein folding (reviewed in Ferrari and Soling, 1999). However, in some cases they appear to prefer different substrates (Cotterill et al., 2005; Koivunen et al., 1996; Kramer et al., 2001; Papp et al., 2006; Zhang et al., 2006) or different folding intermediates of a specific substrate (Satoh et al., 2005). Whether PDI, ERp57, and ERp72 have similar or diverse functions during ER quality control is unknown. We therefore compared their abilities to facilitate retrotranslocation (Chapter 2). In contrast to PDI's ability to facilitate CTA1 retrotranslocation, ERp72 retains the toxin in the ER, and ERp57 does not appear to function in either pathway. Moreover, ERp72 mediates the ER retention of misfolded thyroglobulin and a general population of misfolded proteins destined for ERAD indicating that it functions generally in this process. Consistent with the opposing effects of PDI and ERp72 on the toxin's retrotranslocation, we found that ERp72 stabilizes a folded conformation of CTA1 in contrast to PDI's ability to unfold the toxin (Chapter 2). We conclude that PDI, ERp72, and ERp57 have diverse functions during ER quality control.

Given the similar structures of PDI, ERp57, and ERp72 (Fig. 1.3), we hypothesized that some of their functional differences lie within their corresponding thioredoxin-like domains. To test this, we generated PDI-ERp72 and PDI-ERp57 hybrid proteins and assessed their abilities to unfold CTA1 *in vitro* (Chapter 3). The results of these experiments indicate that most of their thioredoxin-like domains are not interchangeable in the unfolding reaction; thus, some of these domains are functionally unique despite having similar tertiary structures.

Collectively, the work presented here elucidates components of the quality control machinery important for both ERAD and toxin trafficking and provides insight into mechanisms underlying these processes. In addition, these studies demonstrate that PDI family proteins have unique functions during ER quality control and suggest the molecular basis for this diversity lies within unique features of their corresponding thioredoxin-like domains. Thus, these studies enhance our understanding of ER quality control and elucidate functional differences among PDI family proteins.

Figure 1.1 Crystal structure of cholera toxin.
Cholera toxin comprises a single A subunit (CTA) and a ring-shaped homopentameric B subunit (CTB) joined noncovalently. Upon secretion from the bacterium *Vibrio cholerae*, CTA is cleaved into the A1 and A2 polypeptides, which are joined by a disulfide bond and noncovalent interactions. Figure adapted from Zhang et al. (2006).

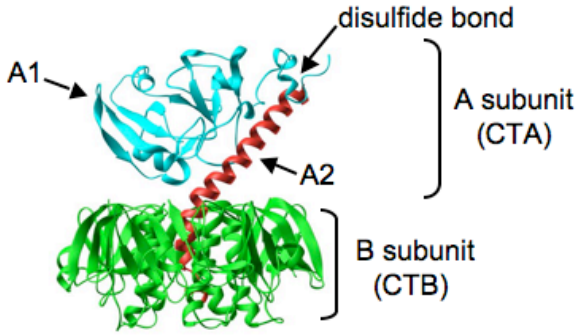

Figure 1.2 Intracellular trafficking of cholera toxin.
CTB binds the ganglioside GM1 on the surface of a host cell, and the holotoxin undergoes retrograde transport through the secretory pathway to the ER lumen. In the ER, the disulfide bond joining CTA1 and CTA2 is reduced, the subunits disassemble, and CTA1 is presumably unfolded. Unfolded CTA1 undergoes retrotranslocation through a protein channel in the ER membrane that appears to include Derlin-1, while CTB remains in the ER. In the cytosol, CTA1 refolds and activates a cAMP-dependent signal cascade that results in chloride secretion.

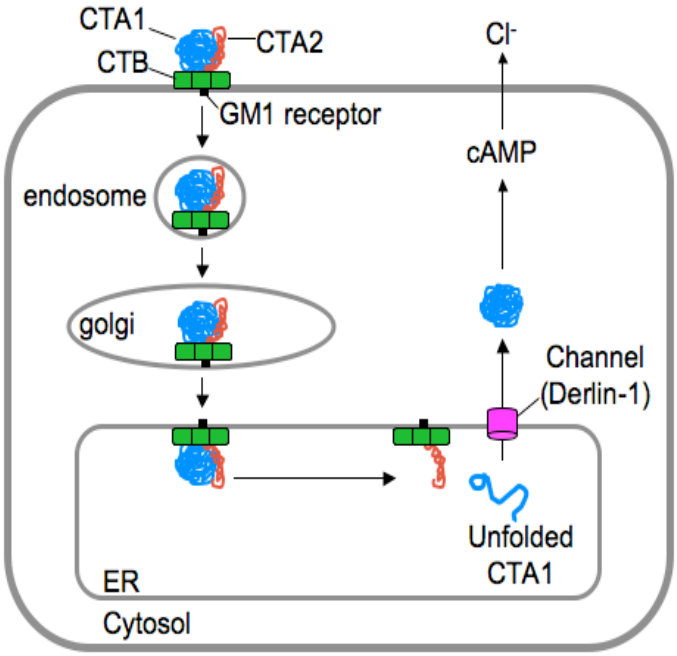

Figure 1.3 The human protein disulfide isomerase family.
Thioredoxin-like domains are depicted by rectangles with the active site sequences of the a-type domains indicated. The linker region (x) between the b' and a' domains is colored grey and transmembrane domains are colored red. Orange bars represent regions of undetermined structure. Figure adapted from Ellgaard and Ruddock (2005).

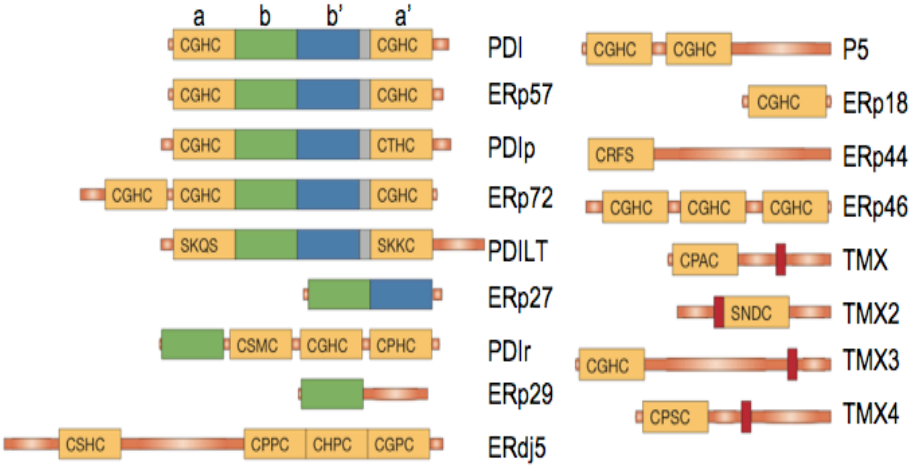

Chapter 2

Protein Disulfide Isomerase Family Proteins Play Opposing Roles during Quality Control in the Endoplasmic Reticulum

Introduction

ER resident proteins facilitate the folding of nascent polypeptides destined for the secretory pathway. Nevertheless, it is common for proteins to misfold (reviewed in Goldberg, 2003). Because misfolded proteins are potentially harmful to cellular health (reviewed in Ni and Lee, 2007), the ER quality control system retains misfolded proteins in the organelle to prevent them from reaching their target destinations and perhaps to allow additional attempts at proper folding (reviewed in Ellgaard and Helenius, 2003). Terminally misfolded proteins are retrotranslocated to the cytosol for degradation by the ubiquitin-dependent proteasome, a process known as ER-associated degradation (ERAD) (reviewed in Tsai et al., 2002). In addition to misfolded proteins, several viruses and toxins that invade mammalian cells use the host cell's quality control system to exert their pathogenic effects (reviewed in Tsai et al., 2002). Because of the relevance of ER quality control to human health, we undertook this study to identify factors that facilitate this process using the catalytic A1 subunit of cholera toxin (CTA1) as a substrate. Because CTA1 has features of a misfolded protein (Zhang et al., 1995) and undergoes retrotranslocation similarly to endogenous misfolded proteins (Bernardi et al., 2008), insights revealed in this study are likely to be applicable to both toxin trafficking and the ERAD pathway.

Previous studies have shown that PDI dissociates the CT holotoxin and unfolds the A subunit (CTA) and CTA1 *in vitro* (Tsai et al., 2001). Because the B subunit (CTB) remains in the ER while CTA1 is active in the cytosol (Fujinaga et al., 2003), dissociation of the holotoxin is required for retrotranslocation. Furthermore, it is possible the toxin

must be unfolded to fit through the retrotranslocation channel (Tsai et al., 2002). Thus, we hypothesized that PDI facilitates the retrotranslocation of CTA1.

Mammalian PDI has also been implicated in the retrotranslocation of ERAD substrates (Gillece et al., 1999; Molinari et al., 2002). Previous studies show that yeast PDI facilitates the ERAD of a mutant secretory protein (Gillece et al., 1999). Moreover, mammalian PDI was shown to associate with a misfolded protein in the ER immediately prior to its degradation in the cytosol (Molinari et al., 2002). Because retrotranslocation is a prerequisite for cytosolic degradation, these studies implicate PDI in the retrotranslocation of ERAD substrates. Therefore, we hypothesized that PDI assists the retrotranslocation of ERAD substrates in addition to CTA1. Our data indicate that mammalian PDI facilitates the retrotranslocation of CTA1, a specific misfolded secretory protein (mutant thyroglobulin), and a general population of ERAD substrates. Thus, this study provides the first functional evidence that mammalian PDI facilitates retrotranslocation and indicates that PDI is a general component of the retrotranslocation machinery.

In addition to PDI, we studied whether two PDI family proteins, ERp57 and ERp72, function in the retrotranslocation pathway. Of the approximately twenty PDI family proteins in mammals, ERp57 and ERp72 most closely resemble PDI in structure (Fig. 2.1) and expression pattern (reviewed in Maattanen et al., 2006). Specifically, PDI comprises two redox active (*a* and *a'*) and two redox inactive (*b* and *b'*) thioredoxin-like domains, a linker (*x*), and an acidic C-terminal extension (*c*) arranged *abb'xa'c* (Edman et al., 1985; Kemmink et al., 1996; Pirneskoski et al., 2004). ERp57 also comprises *abb'xa'c* domains except that its *c* domain contains basic amino acids, whereas ERp72 contains an acidic extension (*c*) and an additional *a* domain at its N-terminus arranged *ca°abb'xa'* (Maattanen et al., 2006). PDI, ERp57, and ERp72 each catalyze oxidative protein folding, albeit with some differences in their substrate specificities (reviewed in Ferrari and Soling, 1999; Maattanen et al., 2006). To further understand the relative functions of each protein, we tested whether ERp72 and ERp57 facilitate retrotranslocation similar to PDI.

To study the retrotranslocation of CT, we developed a semi-permeabilized cell system that monitors the amount of CTA1 in the cytosol. We then used this assay to test the effect of siRNA-mediated down-regulation of PDI, ERp57, or ERp72 protein expression on the toxin's retrotranslocation. We found that PDI facilitates the toxin's retrotranslocation, whereas ERp72 retains the toxin in the ER, and ERp57 appears to be neutral in both processes. Moreover, we found the opposing functions of PDI and ERp72 operate on endogenous proteins misfolded in the ER, indicating the generality of their functions. Thus, in addition to demonstrating PDI's role in retrotranslocation, this study establishes an assay to study CTA1 retrotranslocation and indicates that PDI family proteins play opposing roles during ER quality control.

Results

Retrotranslocation of CTA1

We developed an assay to monitor the retrotranslocation of CTA1 from the ER into the cytosol based on a semi-permeabilized cell assay that efficiently separates cytosolic proteins from ER proteins (Le Gall et al., 2004). After intoxication with CT, HeLa cells were treated with 0.04% digitonin to permeabilize the plasma membrane and then fractionated by centrifugation. The supernatant fraction should contain cytosolic proteins and retrotranslocated CTA1, whereas the pellet fraction should contain the plasma membrane, intracellular organelles (including the ER), and toxin that did not undergo retrotranslocation. We tested the purity of these fractions and found the ER-resident protein ERp57 entirely in the pellet (Fig. 2.2A, second panel from bottom, even lanes), whereas the cytosolic protein Hsp90 was mostly in the supernatant (Fig. 2.2A, bottom panel, odd lanes). When we intoxicated cells at 37°C, a portion of CTA1 appeared in the supernatant (Fig. 2.2A, top panel, compare lane 6 to 5), whereas CTB was only in the pellet fraction (Fig. 2.2A, second panel from top, compare odd to even lanes) as expected. Typically, 15-30% of toxin and less than 0.01% of ER-resident proteins were detected in the supernatant (calculation not shown), indicating the presence of CTA1 in this fraction was not due to ER leakage. This range is likely due to the variable efficiency of the low level of detergent used in this study to permeabilize the plasma membrane. When we incubated cells with CT at 4°C or in the presence of brefeldin A (BFA) at

37°C, which blocks the toxin's arrival to the ER (Fujinaga et al., 2003), CTA1 did not appear in the supernatant (Fig. 2.2A, top panel, compare lane 5 to lanes 1 and 3). Because cell permeabilization in the presence of the alkylating reagent N-ethylmaleimide (NEM) diminished the appearance of CTA1, we believe that a portion of CTA in the pellet was reduced post-lysis (Fig. 2.2A, compare lane 10 to 8). However, the level of CTA1 in the supernatant is similar regardless of whether NEM is present in the lysis buffer (Fig. 2.2A, compare lane 9 to 7). Thus, post-lysis reduction of CTA in the pellet does not trigger the release of CTA1 to the supernatant.

We characterized this assay further by assessing the fractionation pattern of a CT mutant whose A subunit cannot be cleaved due to a mutation at the cleavage site (CT-R192H). Chloride secretion triggered by the R192H mutant is attenuated dramatically (Lencer et al., 1997), indicating this toxin does not undergo retrotranslocation efficiently. As expected, no toxin appeared in the supernatant of cells incubated with CT-R192H (Fig. 2.2B, compare lane 3 to 1).

CT-stimulated chloride secretion is resistant to proteasome inactivation indicating the toxin escapes proteasomal degradation in the cytosol (Rodighiero et al., 2002). Accordingly, inhibition of the proteasome with MG132, confirmed by the accumulation of poly-ubiquitinated proteins (Fig. 2.2C, compare lane 2 to 1), did not significantly change the amount of CTA1 found in the cytosol (Fig. 2.2C, top panel, compare lane 5 to 3). The consistency of these results (Fig. 2.2) with previous chloride secretion studies validates the use of this semi-permeabilization assay as a tool to study CTA1 retrotranslocation directly.

Down-regulation of PDI-like proteins

To study the functions of PDI, ERp72, and ERp57 during CTA1 retrotranslocation, we first down-regulated their protein expression levels using siRNA. Cells transfected with siRNA directed against PDI (PDI$^-$), ERp72 (ERp72$^-$), or ERp57 (ERp57$^-$) mRNA displayed reduced levels of the corresponding proteins (Fig. 2.3A, top panels); in each case, expression of other PDI-like proteins was unaffected (Fig. 2.3A, bottom three

panels). Thus, the protein expression of PDI, ERp57, and ERp72 can be reduced efficiently and specifically.

To ensure that down-regulation of the PDI-like proteins did not globally disrupt ER function, we tested whether their down-regulation elicited the unfolded protein response (UPR). The UPR is a cellular stress response in which the accumulation of misfolded proteins in the ER leads to increased expression of ER chaperones, such as BiP, to alleviate protein misfolding (reviewed in Schroder and Kaufman, 2005). BiP expression was only up-regulated marginally in PDI$^-$, ERp72$^-$, and ERp57$^-$ cells compared to wild-type cells (Fig. 2.3B, compare lanes 3, 5, and 7 to 1), indicating the lack of these proteins did not significantly induce the UPR. Moreover, when we incubated wild-type, PDI$^-$, ERp72$^-$, and ERp57$^-$ cells with tunicamycin, a drug that blocks N-glycosylation causing the accumulation of misfolded proteins, BiP expression was increased in each cell type (Fig. 2.3B, compare lane 2 to lanes 4, 6, and 8) indicating the UPR can be induced in these cells. We conclude that down-regulation of PDI, ERp72, or ERp57 does not globally disrupt ER function.

PDI and ERp72 play opposing roles during CT retrotranslocation

We assessed the effect of PDI down-regulation on the retrotranslocation of CTA1 using our semi-permeabilized cell system. When cells were intoxicated for 45 or 90 min, we found a decreased level of CTA1 (and CTA) in PDI$^-$ cells compared to wild-type cells (Fig. 2.4A, top panel, compare lane 2 to 1 and lane 4 to 3, and quantified below). These data indicate that PDI facilitates the toxin's retrotranslocation, consistent with our hypothesis that PDI-dependent unfolding of CTA1 mediates the toxin's retrotranslocation (Tsai et al., 2001). We note that a low level of CTA also appeared in the supernatant. This is unlikely due to ER leakage as ER markers and CTB were absent from this fraction. Thus it is possible that, whereas CTA1 is the preferred retrotranslocation substrate, CTA also undergoes retrotranslocation, but with lower efficiency.

In contrast to PDI's ability to facilitate CTA1 retrotranslocation, more CTA1 (and CTA) appeared in the supernatant of ERp72$^-$ cells compared to wild-type cells (Fig. 2.4A, top

panel, compare lane 6 to 5 and lane 8 to 7, and quantified below), suggesting that ERp72 retains CTA1 in the ER. The effects of down-regulating PDI and ERp72 on toxin transport were also observed when NEM was present in the lysis buffer (not shown). In contrast to PDI and ERp72, down-regulation of ERp57 did not affect CTA1 retrotranslocation (Fig. 2.4A, top panel, compare lane 10 to 9 and lane 12 to 11). We conclude that the opposing effects of PDI and ERp72 on CTA1 retrotranslocation are specific and unlikely due to a general disruption of ER chaperone functions.

To show that PDI and ERp72 down-regulation did not affect CT trafficking to the ER, we tested whether a variant of CT containing N-glycosylation sites in the B subunit (CT-GS) became glycosylated in PDI^- and $ERp72^-$ cells. Modification by N-glycosylation, detected by a molecular mass increase in CTB that is sensitive to N-glycanase, indicates the toxin's arrival to the ER (Fujinaga et al., 2003). When cells were intoxicated with CT-GS at 37°C and analyzed by SDS-PAGE of cellular lysates followed by immuno-blotting with an anti-CTB antibody, a higher molecular weight band representing glycosylated CTB was observed (Fig. 2.4B, lane 2). Glycosylated CTB was not detected in cells incubated with the toxin at 4°C or in the presence of BFA at 37°C (Fig. 2.4B, lanes 1 and 3). These experiments validate the use of CT-GS in monitoring the arrival of CTA to the ER. Significantly, the similar level of glycosylated CTB found in wild-type, PDI^-, and $ERp72^-$ cells (Fig. 2.4B, lanes 4-6) indicates that PDI and ERp72 act on the toxin only after it reaches the ER. Furthermore, PDI and ERp72 down-regulation does not affect the reduction of CTA (Fig. 2.4C, compare lane 2 to 1 and lane 4 to 3).

Upon reaching the cytosol, CTA1 ADP-ribosylates the Gαs protein, activating adenylate cyclase that then generates cAMP. We therefore measured the CT-induced cAMP response in PDI^- and $ERp72^-$ cells. CT triggered the production of 50% less cAMP in PDI^- cells than in wild-type cells (Fig. 2.4D, left graph). Forskolin, which stimulates adenylate cyclase directly, elicited a similar cAMP level in wild-type and PDI^- cells (not shown), indicating that PDI down-regulation did not affect adenylate cyclase. In contrast, CT induced the production of 40% more cAMP in $ERp72^-$ cells than in wild-type cells (Fig. 2.4D, right graph). This result was normalized against the forskolin-induced cAMP

response because forskolin also triggered a higher cAMP response in ERp72$^-$ cells than in wild-type cells; the higher forskolin-induced cAMP response in these cells is likely due to a concomitant increase in cell surface expression of adenylate cyclase (not shown). These data are consistent with data from the retrotranslocation assay showing that PDI facilitates CTA1 retrotranslocation whereas ERp72 retains the toxin in the ER.

Opposing effects of PDI and ERp72 on the conformation of CT

PDI's ability to unfold CTA and CTA1 (Tsai et al., 2001) is consistent with its role in the toxin's retrotranslocation. ERp72's ability to retain the toxin in the ER suggests that it may recognize CT as a misfolded protein and attempt to "refold" the toxin's structure. We tested this hypothesis using a trypsin-sensitivity assay to monitor the conformation of CTA1 (and CTA) when incubated with PDI or ERp72. As reported previously, incubation of purified PDI but not the control protein bovine serum albumin (BSA) with CTA under reducing conditions rendered CTA and CTA1 sensitive to tryptic-digestion (Fig. 2.5B, compare lane 2 to 1; Tsai et al., 2001), indicating PDI unfolded the toxin. In contrast, purified ERp72 (Fig. 2.5A) did not cause the toxin to become trypsin-sensitive (not shown). Using a higher trypsin concentration that renders the toxin sensitive to degradation in the absence of PDI (Fig. 2.5B, compare lanes 3 and 4 to 1), ERp72 protected the toxin from degradation (Fig. 2.5B, compare lane 5 to 3 and 4), indicating that ERp72 stabilizes a folded conformation of CTA1 and CTA. Thus, PDI and ERp72's opposing effect on the conformation of CT correlates with their opposing roles in ER quality control.

General roles for PDI and ERp72 during ER quality control

We next asked whether the opposing functions of PDI and ERp72 represent a general mechanism operating in the ER. To test this, we developed a method to measure the bulk arrival of misfolded proteins from the ER to the cytosol. Misfolded polypeptides undergoing retrotranslocation are poly-ubiquitinated upon reaching the cytosolic surface of the ER membrane, which targets them for proteasomal degradation (reviewed in Tsai et al., 2002). Consequently, inactivation of the proteasome should cause the accumulation of poly-ubiquitinated proteins from the ER (in addition to poly-ubiquitinated cytosolic

proteins). Therefore, the effect of down-regulating an ER-resident protein on the accumulation of total poly-ubiquitinated proteins should reflect its role in retrotranslocation. We measured the level of poly-ubiquitinated proteins and found that incubation of cells with the proteasome inhibitor MG132 resulted in an increase of poly-ubiquitinated proteins (Fig. 2.6A, compare lane 3 to 1 and lane 7 to 5). When PDI$^-$ cells were treated with MG132, fewer poly-ubiquitinated proteins appeared in these cells than in MG132-treated wild-type cells (Fig. 2.6A, compare lane 4 to 3, and quantified below). In contrast, more poly-ubiquitinated proteins appeared in ERp72$^-$ cells (Fig. 2.6A, compare lane 8 to 7, and quantified below). Quantification shows that PDI down-regulation reduced the total level of poly-ubiquitinated proteins by approximately 40%, whereas 60% of poly-ubiquitinated proteins were unaffected. These unaffected proteins presumably originated from the cytosol rather than the ER.

We next tested whether the ubiquitin-proteasome system is affected non-specifically by down-regulating PDI or ERp72 using IκBα as a substrate. IκBα is a cytosolic protein that is poly-ubiquitinated in response to tumor necrosis factor-alpha (TNFα) stimulation, leading to the proteasomal degradation of IκBα (reviewed in Karin and Ben-Neriah, 2000). When wild-type, PDI$^-$, and ERp72$^-$ cells were treated with TNFα, IκBα was degraded with similar efficiency in each cell type (Fig. 2.6B, compare lanes 4, 5, and 6 to 1, 2, and 3), indicating that IκBα ubiquitination and proteasomal degradation was not disrupted by PDI and ERp72 down-regulation. These data suggest the effects of PDI and ERp72 down-regulation on the accumulation of poly-ubiquitinated proteins were not indirectly due to changes in the ubiquitin-proteasome system. Thus, we conclude that PDI facilitates the retrotranslocation of proteins misfolded in the ER, while ERp72 mediates their ER retention, similar to their roles in CTA1 retrotranslocation.

We additionally examined the roles of PDI and ERp72 in the retrotranslocation of a specific protein misfolded in the ER. Thyroglobulin (Tg), the thyroid prohormone, is folded in the ER before being secreted. A mutant form of Tg, cogTg, was shown previously to undergo ERAD (Tokunaga et al., 2000). Over-expression of PDI in CHO cells stably expressing cogTg (CHO-PDI) stimulated the rate of cogTg degradation

compared to parental CHO cells expressing cogTg (CHO-P) (Fig. 2.6C, compare open to closed squares). In contrast, over-expression of ERp72 (CHO-ERp72) decreased the rate of cogTg degradation (Fig. 2.6C, compare open squares to circles). These results suggest that PDI stimulates the retrotranslocation of cogTg while ERp72 retains it in the ER. We conclude that PDI and ERp72's opposing roles operate not only on CTA1 retrotranslocation, but also on endogenous proteins misfolded in the ER.

Discussion

The data presented here indicates that PDI facilitates the retrotranslocation of CTA1 and ERAD substrates. Because PDI unfolds the toxin *in vitro*, our results imply that unfolding is a prerequisite for efficient retrotranslocation. Indeed, studies show that folded proteins cannot be translocated across ER (Schlenstedt et al., 1994), lysosomal (Salvador et al., 2000), or mitochondrial membranes (Eilers and Schatz, 1986) ostensibly due to the narrow size and limited flexibility of their protein-conducting channels (reviewed in Schnell and Hebert, 2003). Specifically, a stably folded protein attached to the A subunit of ricin, a toxin related to CT, hindered the toxin's retrotranslocation into the cytosol (Beaumelle et al., 1997). Together, these studies indicate that unfolding might be a general prerequisite for retrotranslocation. Whether all substrates are unfolded by PDI or additional unfoldases exist in the ER remains to be determined.

In contrast to PDI, ERp72 retains CTA1 and ERAD substrates in the ER. ER retention is a quality control mechanism that ensures misfolded proteins do not reach their target destinations (reviewed in Ellgaard and Helenius, 2003). Retention by ERp72 correlates with its ability to stabilize a folded conformation of the toxin. Whether ERp72 stabilizes the toxin's native conformation or renders it more compactly folded is unclear. Regardless, this result suggests that ERp72 might attempt to correctly fold proteins during their retention.

The opposing effects of PDI and ERp72 on the conformation of CT correlates with their respective roles in retrotranslocation versus ER retention. Similarly, PDI but not ERp72 facilitates the unfolding of a non-native intermediate of bovine pancreatic trypsin

inhibitor during isomerization of the substrate's disulfide bonds (Satoh et al., 2005). Furthermore, ERp72 but not PDI was found associated with a misfolded secretory protein (Cotterill et al., 2005) and a misfolded transmembrane protein (Sorensen et al., 2005) that are each retained in the ER. Given their structural homology, how PDI and ERp72 mediate these opposing functions is unclear. Their major differences are that ERp72 contains an additional *a* domain at its N-terminus that is absent in PDI, and PDI's *c* domain is at its C-terminus whereas ERp72's *c* domain is at its N-terminus (Fig. 2.1). It remains to be determined whether these structural variations explain their functional differences.

Our data identifies ERp72 and PDI as factors in ER quality control that are analogous to chaperones that perform quality control in the cytosol (Figure 2.6D; McClellan et al., 2005). The cytosolic chaperones Hsp70 and TriC co-operate to assist protein folding, whereas Hsp70 and the Hsp90/Sti1/Sse1 complex promote the degradation of misfolded proteins. Furthermore, similar to Hsp70, PDI facilitates the degradation of misfolded proteins (shown here), in contrast its ability to promote productive protein folding (reviewed in Wilkinson and Gilbert, 2004). Although PDI does not require partner proteins to perform its multiple activities *in vitro*, it remains to be determined whether partners help PDI choose between functions in the crowded environment of the ER.

Experimental Methods

Materials

Antibodies against PDI, BiP, and Hsp90 were purchased from Santa Cruz, ERp72 from Stressgen, ubiquitin from Zymed, and IκBα from Biolegend. CTA and CTB antibodies and CT-GS were provided by the Lencer lab, the thyroglobulin antibodies from the Arvan lab, and the CT-R192H mutant from R. Holmes (University of Colorado). Hsp27, ERp57, and ERp29 antibodies were generous gifts from M. Welsh (University of Michigan), S. High (University of Manchester), and S. Mkrtchian (Karolinska Intitutet), respectively. CT, CTA, and PDI were purchased from Calbiochem. Mouse ERp72 cDNA was subcloned into pQE30 and the protein purified using a Ni-NTA agarose column.

siRNA-mediate protein down-regulation of protein expression

PDI-specific (5'-GACCTCCCCTTCAAAGTTGTT-3') siRNA was synthesized by Ambion and ERp72-specific (5'-CAAGCGUUCUCCUCCAAUUTT-3') and ERp57-specific (5'-UGAAGGUGGCCG UGAAUUATT-3') siRNAs by Invitrogen. Duplexed siRNA (10 nM) was transfected into HeLa cells using Oligofectamine (Invitrogen) according to the manufacturer's protocol. Protein expression was assessed by SDS-PAGE and immunoblot analysis. Experiments were initiated 48 hrs (ERp57) or 72 hrs (PDI and ERp72) post-transfection.

Retrotranslocation assay

Cells were incubated with CT (10 nM) in Hanks' balanced salt solution (HBSS) at 37°C for 45 or 90 min. For permeabilization, 2 x 10^6 cells were resuspended in 100 ml of 0.04% digitonin in HCN buffer (50 mM HEPES pH 7.5, 150 mM NaCl, 2mM $CaCl_2$ and protease inhibitors) with or without NEM (10 mM), incubated on ice for 10 min and centrifuged at 16,000 g for 10 min. The supernatant was removed and the pellet washed with PBS and resuspended in 100 ml of the original buffer. Fractions were analyzed by non-reducing SDS-PAGE and immunoblot analysis. Where indicated, cells were treated with MG132 (2 mM) for 90 min.

N-Glycosylation of CTB

HeLa cells were incubated with CT-GS (50 nM) in HBSS for 3 h at 4°C, or 37°C in the presence or absence of BFA (5 mg/ml). Cells were harvested in TN lysis buffer (1% Triton X-100, 1.75% n-octyl-B-/d-glucopyranoside, 10 mM Tris pH 7.4, 150 mM NaCl, 5 mM EDTA, protease inhibitors), and the lysates analyzed for the presence of glycosylated CTB.

cAMP assay

A cAMP enzyme-immunoassay system (Amersham) was used to quantify cAMP synthesis induced by CT (10 nM) or forskolin (FK, 50 mM) in HBSS. Samples were assayed in duplicate, and the average optical density was used to calculate the cAMP level/well. The cAMP response was determined by dividing the cAMP level in CT- or

FK-treated cells by the cAMP level in unstimulated cells. Forskolin induced a seven-fold higher cAMP response in ERp72^{-} cells than in wild-type cells. Results are reported as a percentage of the wild-type CT-induced cAMP response normalized to the FK-induced cAMP response.

Trypsin-sensitivity assay

Purified CTA was incubated with GSH (1 mM), BSA (2 mg/ml), PDI (2 mg/ml), or ERp72 (0.2 mg/ml) for 30 min at 37°C. Trypsin (100 mg/mL or 300 mg/mL) was added to the samples for 30 min at 4°C. Samples were analyzed by nonreducing SDS-PAGE followed by immunoblot analysis.

Accumulation of poly-ubiquitinated proteins

Cells were incubated with or without MG132 (20 mM) for 30 min, lysed in a buffer containing 1% Triton-X, 10 mM NEM, 30 mM HEPES pH 7.4, 150 mM NaCl, 5 mM EDTA, and protease inhibitors. Cleared lysates were analyzed by 4-20% SDS-PAGE followed by immunoblot analysis. To monitor ubiquitin-dependent degradation of IκBα, cells were treated with TNFα (10 ng/mL) for 15 min and the cell lysate analyzed for the presence of IκBα.

Pulse-chase analysis

Cog Tg degradation rate was analyzed as previously described (Tokunaga et al., 2000).

Figure 2.1 Diagram of the domain compositions of PDI, ERp72, and ERp57.
Thioredoxin-like domains are represented by rectangles. The redox active domains are indicated by the presence of the CGHC sequence (*a°*, *a*, and *a'*), whereas the redox inactive thioredoxin-like domains (*b* and *b'*) lack this sequence. The flexible region linking the b' and a' domains is denoted by "x." Boxes with diagonal lines represent an acidic extension (*c* domain), whereas speckled boxes represent a basic extension.

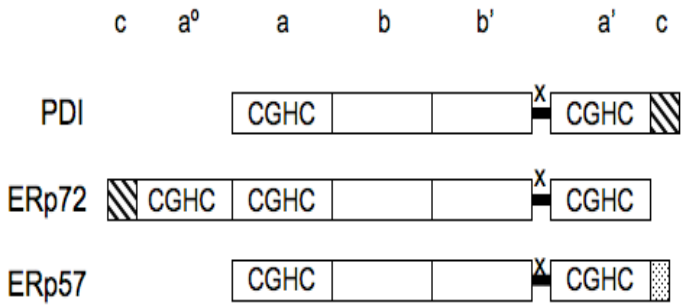

Figure 2.2 Retrotranslocation of CTA1.
A. HeLa cells were incubated with CT for 90 min at 4°C or 37°C with or without BFA or NEM. Cell membranes were permeabilized followed by centrifugation. The resulting supernatant and pellet fractions were subjected to non-reducing SDS-PAGE and immunoblotted with the indicated antibodies. B. As in A except a CT mutant, R192H, was used. C. (Left) Cells were treated with or without MG132 and lysates were blotted with an anti-ubiquitin antibody. (Right) As in A, except cells were treated with MG132 as indicated.

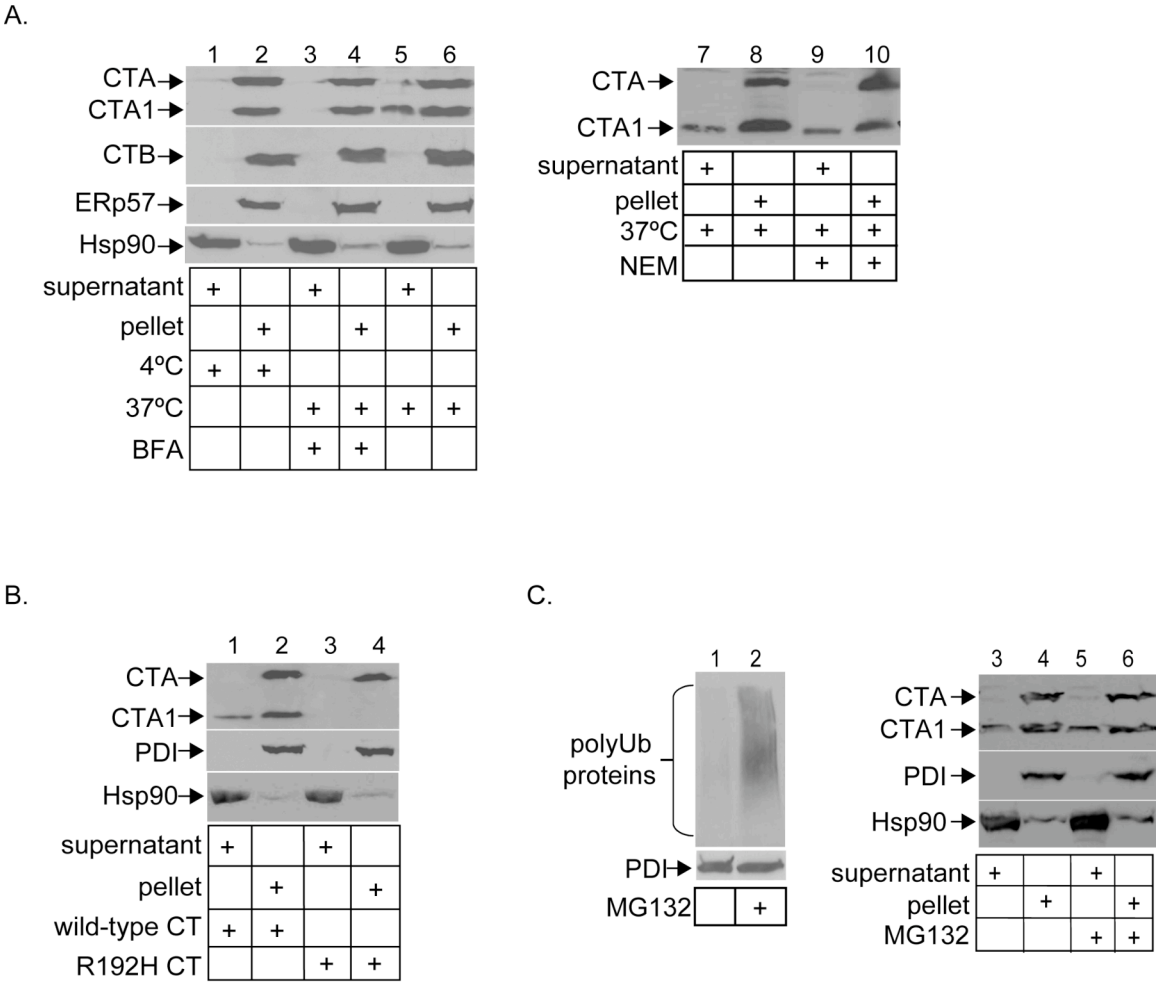

Figure 2.3 Down-regulation of PDI family proteins.
A. PDI, ERp72, ERp57, and ERp29 protein levels were examined in wild-type HeLa cells or cells transfected with siRNA targeting PDI (PDI$^-$), ERp72 (ERp72$^-$), or ERp57 (ERp57$^-$). B. Wild-type, PDI$^-$, ERp72$^-$, and ERp57$^-$ cells were incubated with tunicamycin (Tm) for 8 hrs and BiP expression assessed by SDS-PAGE and immuno-blot analysis.

A.

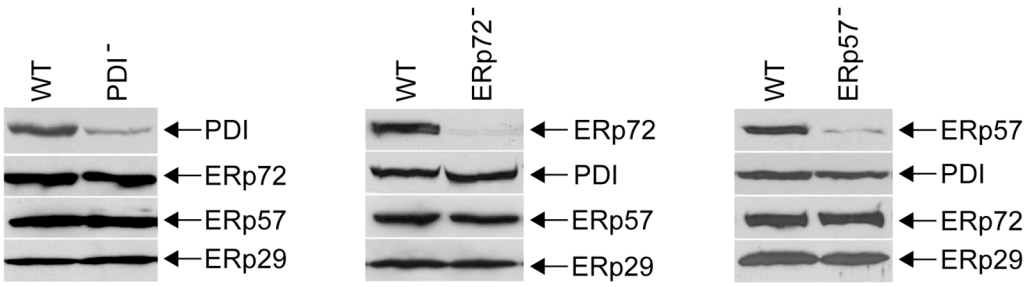

B.

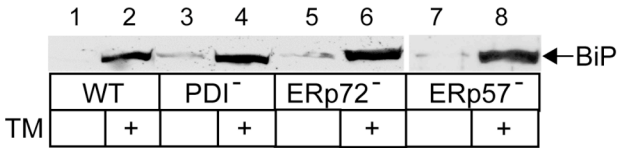

Figure 2.4 PDI and ERp72 play opposing roles during CT retrotranslocation.
A. (top) Wild-type, PDI$^-$, ERp72$^-$, and ERp57$^-$ cells were incubated with CT for 45 or 90 min, permeabilized, and the supernatant fraction analyzed as in Figure 1. (bottom) The intensities of the CTA1 (and CTA) bands in the supernatant were quantified. Graphs show the mean ± S.D. of 2-4 experiments. B. Wild-type, PDI$^-$, and ERp72$^-$ cells were incubated with CT-GS and cell lysates were analyzed by SDS-PAGE followed by immunoblotting with an anti-CTB antibody. Non-glycosylated and glycosylated CTB are 17 kDa and 21 kDa, respectively. C. Whole cell lysates from CT-intoxicated wild-type, PDI$^-$, and ERp72$^-$ cells were prepared in the presence of NEM and analyzed by SDS-PAGE and immunoblotting with an anti-CTA antibody. D. Wild-type, PDI$^-$, and ERp72$^-$ cells were incubated with CT for 90 min and the cAMP level measured by a commercially available kit (Amersham). The means ± S.D. of 2-4 experiments are shown. White lines indicate that intervening lanes were removed.

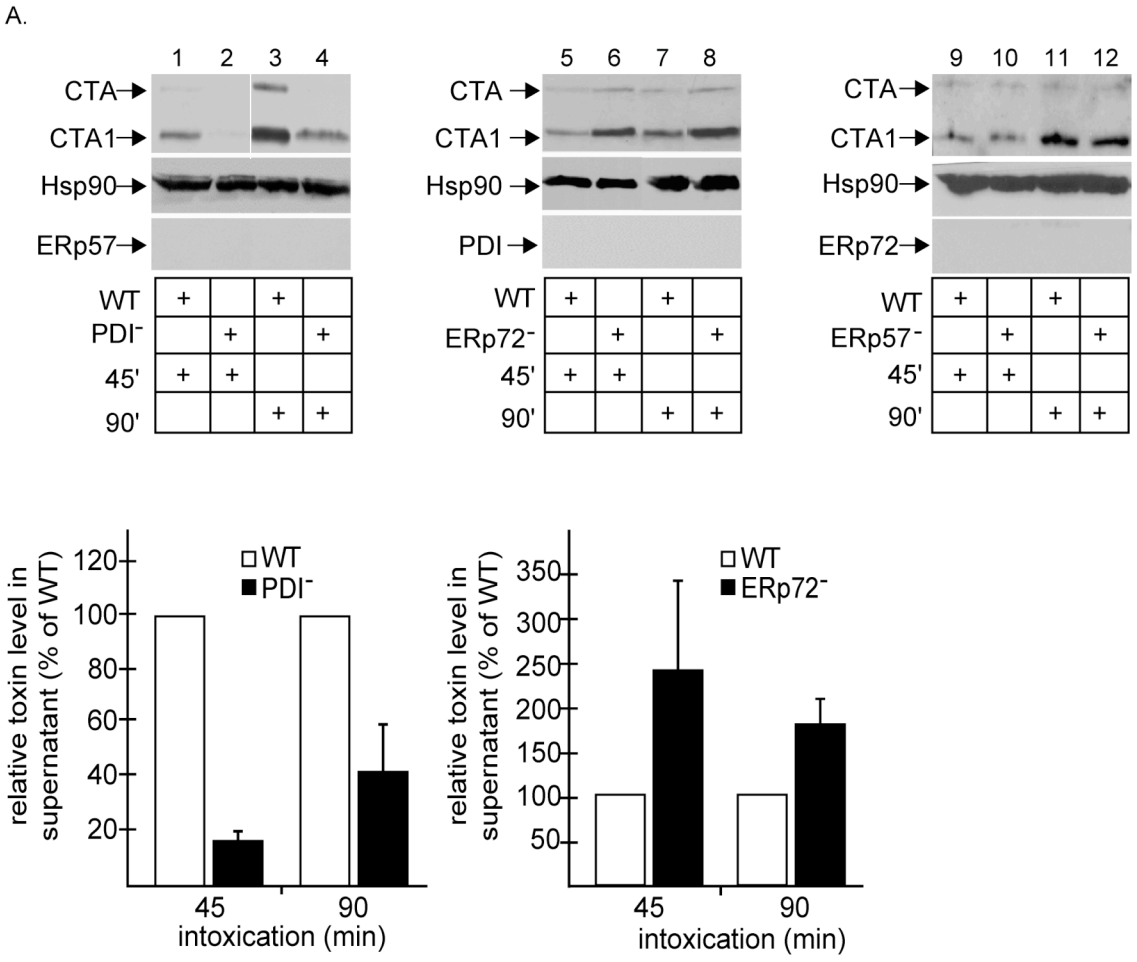

B.

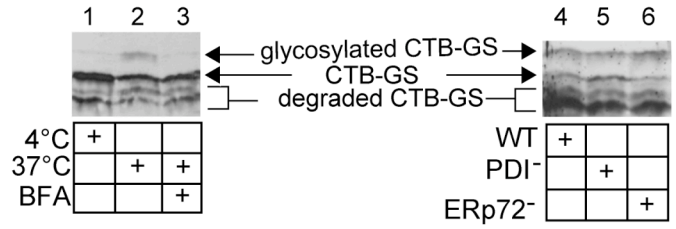
1 2 3
4 5 6
glycosylated CTB-GS
CTB-GS
degraded CTB-GS
4°C
37°C
BFA
WT
PDI-
ERp72-

C.

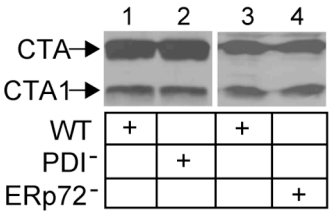
1 2 3 4
CTA
CTA1
WT
PDI-
ERp72-

D.

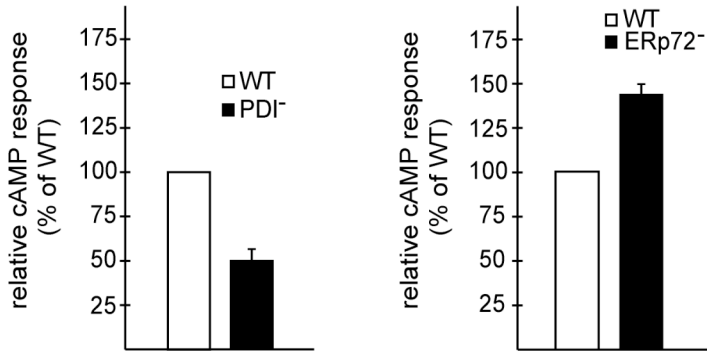
relative cAMP response (% of WT)
175
150
125
100
75
50
25
WT
PDI-
WT
ERp72-

Figure 2.5 PDI and ERp72 exert opposing effects on the conformation of CT.
A. His-tagged ERp72 protein was purified from bacteria and analyzed by SDS-PAGE followed by Coomassie staining or immunoblotting with an antibody against ERp72. B. CTA was incubated with BSA, PDI, or ERp72 followed by the addition of trypsin. Samples were subjected to SDS-PAGE followed by immunoblotting with an anti-CTA antibody.

A.

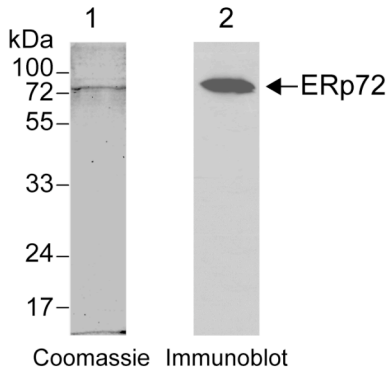

B.

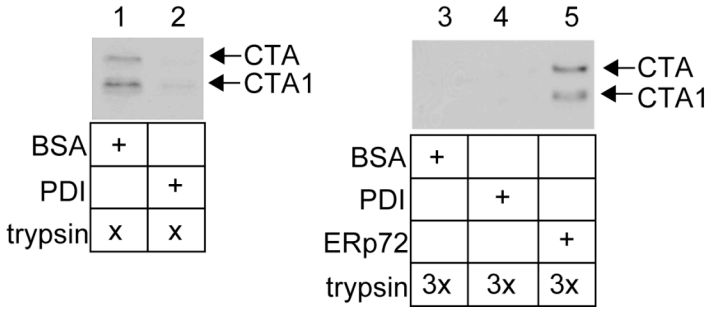

Figure 2.6 General roles for PDI and ERp72 during ER quality control.
A. (top) Wild-type, PDI$^-$, or ERp72$^-$ cells were treated with MG132 and cell lysates were analyzed by SDS-PAGE followed by immunoblotting with the indicated antibodies. (bottom) The total ubiquitin signal intensity was measured. Graphs show the mean ± S.D. of 3-5 experiments. B. Wild-type, PDI$^-$, or ERp72$^-$ cells were treated with TNFα and lysates were analyzed by SDS-PAGE followed by immunoblotting with an antibody against IκBα. C. CHO cells stably expressing cogTg (CHO-P) and PDI (CHO-PDI) or ERp72 (CHO-ERp72) were pulse-labeled with ^{35}S-Met and chased for the times indicated. CogTg was immunoprecipitated from cell lysates with anti-Tg antibody and analyzed by SDS-PAGE. Quantification of the radioactive cogTg band intensity is shown. D. Diagram depicting the similarity between the quality control system in the ER and cytosol. See text for discussion. White lines indicate that intervening lanes were removed.

A.

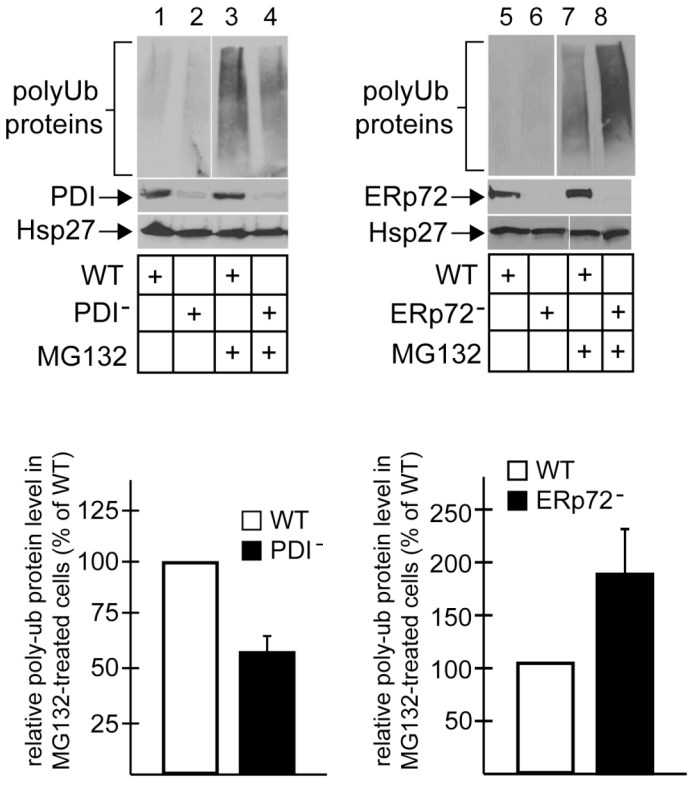

B.

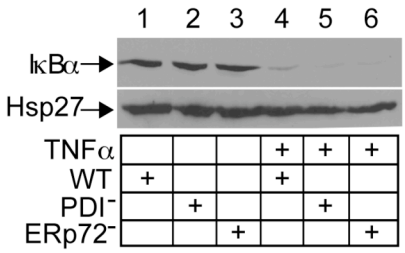
1 2 3 4 5 6
IκBα
Hsp27
TNFα + + +
WT + +
PDI⁻ + +
ERp72⁻ + +

C.

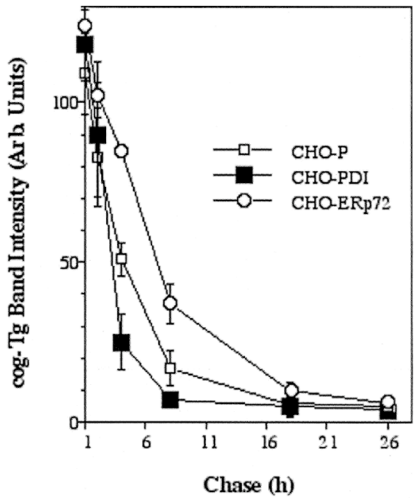
cog-Tg Band Intensity (Arb Units)
100
50
0
1 6 11 16 21 26
Chase (h)
CHO-P
CHO-PDI
CHO-ERp72

D.

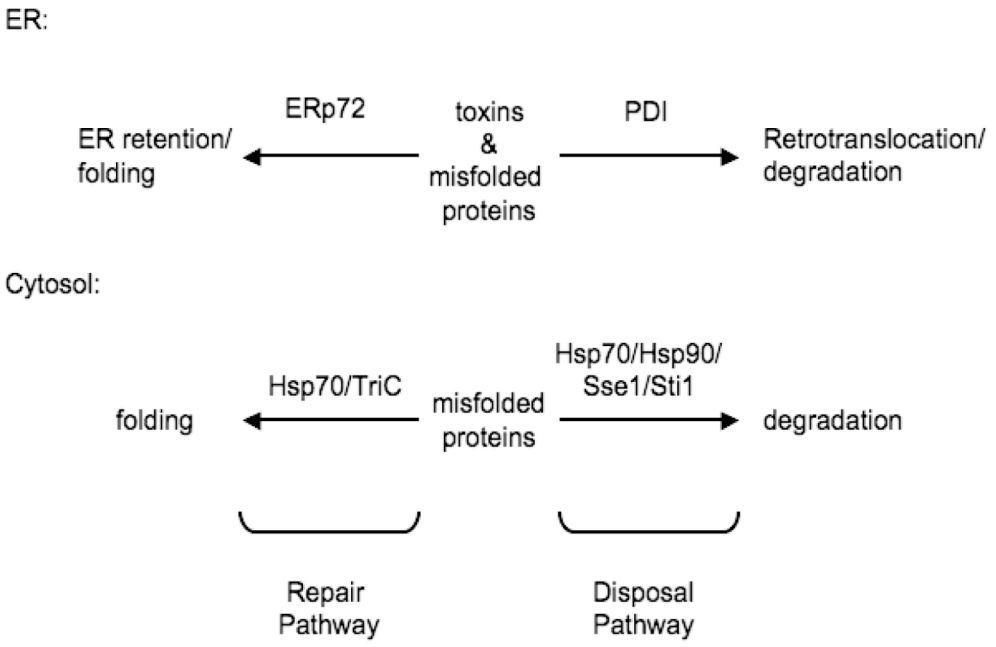
ER:
ERp72
toxins & misfolded proteins
PDI
ER retention/ folding
Retrotranslocation/ degradation
Cytosol:
Hsp70/TriC
Hsp70/Hsp90/ Sse1/Sti1
folding
misfolded proteins
degradation
Repair Pathway
Disposal Pathway

Chapter 3

Generating an Unfoldase from Thioredoxin-like Domains

Introduction

Protein disulfide isomerase (PDI) is a multifunctional protein that resides in the endoplasmic reticulum (ER) lumen of all eukaryotic cells (reviewed in Ferrari and Soling, 1999). It was first identified as catalyst of oxidative protein folding (Goldberger et al., 1964), but is now known to facilitate a variety of other cellular processes, such as viral infection (Gilbert et al., 2006; Schelhaas et al., 2007), antigen processing (Park et al., 2006), and collagen assembly (Pihlajaniemi et al., 1987). During these processes, PDI catalyzes the formation (oxidation) and/or rearrangement (isomerization) of disulfide bonds or functions as a chaperone, binding nonnative proteins to prevent their aggregation, independent of redox activity (Song and Wang, 1995; Wang and Tsou, 1993; Winter et al., 2002). PDI is also a structural subunit of the prolyl 4-hydroxylase complex (P4H; Pihlajaniemi et al., 1987) and microsomal triglyceride transfer protein complex (MTP; Wetterau et al., 1990); however, this role is similar to its function as a chaperone (Lamberg et al., 1996; Vuori et al., 1992a; Vuori et al., 1992b; Wetterau et al., 1991). In contrast to these activities, PDI unfolds the catalytic A1 polypeptide of CT (CTA1) in preparation for the toxin's retrotranslocation from the ER lumen into the cytosol (Forster et al., 2006; Tsai et al., 2001).

PDI was previously shown to act as a redox-dependent chaperone to unfold CTA1 *in vitro* (Tsai et al., 2001). In PDI's reduced state, it binds and unfolds the toxin. Subsequent oxidation of PDI by the ER oxidase Ero1 causes PDI to release unfolded CTA1 (Tsai and Rapoport, 2002). Aside from this information, nothing is known about the mechanism of PDI's unfolding activity.

PDI is a modular protein comprising two a-type thioredoxin-like domains (*a* and *a'*), two b-type thioredoxin-like domains (*b* and *b'*), a flexible linker (*x*), and a C-terminal extension (*c*) arranged *abb'xa'c* (Edman et al., 1985; Kemmink et al., 1996; Pirneskoski et al., 2004). The a-type domains are characterized by the presence of the redox active CXXC sequence, whereas the b-type domains lack this sequence and are therefore redox inactive (Kemmink et al., 1997). Furthermore, PDI's thioredoxin-like domains differ from each other in primary structure despite their similar tertiary structures (Edman et al., 1985). The crystal structure of yeast PDI shows the *bb'* domains form a rigid base from which the a-type domains extend like flexible arms (Tian et al., 2008; Tian et al., 2006). This base is thought to be the core of a substrate-binding groove formed by all four thioredoxin-like domains (Kemmink et al., 1996; Klappa et al., 1998; Tian et al., 2006).

To gain insight into the mechanism of PDI's unfoldase activity, we analyzed the contribution of each domain to PDI's ability to bind and unfold CTA1 using recombinant PDI fragments. Unfolded CTA1 was detected by an established *in vitro* trypsin-sensitivity assay that relies on tryptic cleavage sites hidden in the folded toxin to be exposed in the unfolded toxin (Tsai et al., 2001). We found PDI's linked *bb'xa'* domains are necessary and sufficient to bind and unfold CTA1 efficiently; domains *a* and *c* are not required. The specific linear arrangement of *bb'xa'* and identity of the a-type domain (*a'* versus *a*) C-terminal to *bb'x* are also critical for PDI's unfoldase activity. Together, these data suggest a general mechanism for PDI's unfoldase activity: the concurrent and specific binding of *bb'xa'* to particular regions along the CTA1 molecule triggers its unfolding. Because CTA1 likely mimics a misfolded host cell protein for its recognition and unfolding by PDI (Hazes and Read, 1997; Tsai et al., 2002; Zhang et al., 1995), this study has implications for how PDI might unfold endogenous misfolded proteins in preparation for their retrotranslocation and subsequent ERAD.

There are approximately twenty mammalian PDI family proteins, each characterized by the presence of one or more thioredoxin-like domains and ER localization (reviewed in Appenzeller-Herzog and Ellgaard, 2008). We previously demonstrated that, in contrast to PDI, the PDI family proteins ERp72 and ERp57 do not facilitate CTA1 retrotranslocation

(Forster et al., 2006). Instead, ERp72 retains CTA1 in the ER and stabilizes a folded conformation of the toxin, whereas ERp57 does not appear to participate in the toxin's retrotranslocation or ER retention (Forster et al., 2006). To understand how these structurally homologous proteins are functionally unique, we generated PDI-ERp72 and PDI-ERp57 hybrid proteins and tested their abilities to unfold CTA1 *in vitro*. Our results reveal that PDI's *bb'* domains are indispensable to the unfolding reaction, whereas the function of its *a'* domain can be partially replaced by the corresponding domain from ERp72 or ERp57. PDI's *bb'* domains were not sufficient to convert full-length ERp57 into an unfoldase because ERp57's *a* domain inhibited toxin binding. Thus, in addition to suggesting a general mechanism for PDI's unfoldase activity, our data indicate that generating an unfoldase from thioredoxin-like domains requires PDI's *bb'(x)* domains followed by an *a'* domain but not preceded by an *a* domain capable of inhibiting binding.

Results

Recombinant PDI unfolds CTA1 efficiently

Endogenous PDI derived from bovine liver was shown previously to unfold the CTA and CTA1 polypeptides, rendering them sensitive to tryptic digestion (Tsai et al., 2001). Using a similar assay, we tested whether full-length mouse PDI (PDI-FL) with an N-terminal 6xHis-tag purified from bacteria (Fig. 3.1A) can unfold CTA1. Hence, we incubated CTA with purified PDI-FL or the control protein bovine serum albumin (BSA) in the presence of the reducing agent glutathione (GSH) at 30°C followed by incubation with trypsin at 4°C. Under this condition, the majority of CTA is reduced by GSH to generate CTA1 (data not shown). The samples were then subjected to SDS-PAGE and immunoblotted with an antibody that detects CTA1. Whereas CTA1 was mostly resistant to proteolysis when incubated with BSA (Fig. 3.1B, compare lane 2 to 1), it became sensitive to tryptic digestion when incubated with PDI-FL, (Fig. 3.1B, compare lane 4 to 3). These findings are consistent with results using endogenous PDI (Tsai et al., 2001) and indicate that recombinant PDI unfolds CTA1 efficiently. Furthermore, when the toxin was incubated with PDI at 4°C instead of 30°C (followed by incubation with trypsin at 4°C), CTA1 was resistant to protease digestion (Fig. 3.1C, compare lane 4 to 2)

as expected for a protein-mediated activity. These experiments establish the feasibility of using recombinant PDI to study PDI's unfoldase activity.

PDI's *bb'xa'* domains form the minimum unit required to unfold CTA1

To determine the domain requirements for PDI's unfoldase activity, we expressed and purified the His-tagged PDI fragments shown in Fig. 3.2A and tested their abilities to render CTA1 trypsin-sensitive. Each fragment was isolated as a soluble protein consistent with previous observations that each thioredoxin-like domain autonomously forms a folded structure (Darby and Creighton, 1995; Darby et al., 1996; Darby et al., 1999). When PDI*abb'xa'* was incubated with the toxin followed by incubation with trypsin, CTA1 was digested efficiently (Fig. 3.2B, compare lane 3 to lanes 1 and 2), indicating domain *c* is not required for unfoldase activity. Subsequent deletion of domain *a'*, generating fragment PDI*abb'x*, resulted in a loss of PDI's ability to render CTA1 trypsin-sensitive (Fig. 3.2B, compare lane 5 to 4), whereas deletion of domain *a*, generating PDI*bb'xa'*, did not affect activity (Fig. 3.2B, compare lane 6 to 4). Thus, domain *a'* but not *a* is required for PDI's unfoldase activity. PDI*ab* did not render CTA1 trypsin-sensitive (Fig. 3.2B, compare lane 7 to 4), as expected. However, in contrast to PDI*bb'xa'*, PDI*b'xa'* did not make CTA1 trypsin-sensitive (Fig. 3.2B, compare lane 8 to 6), indicating domain *b* is required for unfoldase activity. To determine if PDI's domains must be linked to induce unfolding, we assessed whether fragments PDI*ab* and PDI*b'xa'* could cooperate to unfold CTA1 and found they could not (Fig. 3.2C, compare lane 3 to 2). We conclude the linked *bb'xa'* domains form the minimum unit required for efficient unfoldase activity.

A PDI-toxin interaction is necessary but not sufficient to trigger unfolding

To further elucidate the unfolding reaction, we sought to identify the PDI domains that interact with CTA1. Hence, we incubated CTA with PDI*abb'xa'* or a control protein, His-tagged ERp29, under reducing conditions to stimulate unfolding. We then immunoprecipitated PDI*abb'xa'* or ERp29, along with any bound toxin, using an anti-His antibody. Immunoprecipitates were analyzed by SDS-PAGE and Coomassie staining or immunoblotting with an antibody against CTA or PDI. As expected, CTA1 co-

precipitated with PDI*abb'xa'*, but not ERp29 (Fig. 3.3A, compare lane 4 to 3), demonstrating the toxin binds specifically to PDI*abb'xa'*. Repeating the same experiment using the various PDI fragments revealed that PDI*abb'x* and PDI*bb'xa'* bound CTA1 with a similar efficiency as PDI*abb'xa'* (Fig. 3.3B, top panel, compare lanes 8 and 9 to 7), whereas the PDI fragments containing only two domains (PDI*ab*, PDI*b'xa'* and PDI*bb'x*) bound CTA1 less efficiently (Fig. 3.3B, top panel, compare lanes 10-12 to lanes 7-9). There was variability in the relative binding abilities among the fragments containing only two domains (data not shown); however, these fragments consistently co-precipitated less CTA1 than fragments with three domains. These results indicate that each PDI thioredoxin-like domain can interact with CTA1, but either PDI*abb'x* or PDI*bb'xa'* is required for a strong interaction. Because PDI*abb'x* and PDI*bb'xa'* bound to CTA1 with similar efficiencies, whereas only PDI*bb'xa'* unfolded the toxin (Fig. 3.2B), we conclude that an efficient PDI-toxin interaction is required but not sufficient to trigger unfolding.

The reduced but not oxidized state of full-length PDI was shown previously to bind CTA1 (Tsai and Rapoport, 2002; Tsai et al., 2001). To test whether PDI*abb'x* or PDI*bb'xa'* also bind in a redox-dependent manner, we incubated CTA with PDI*abb'x* or PDI*bb'xa'* in the presence of either GSH or oxidized glutathione (GSSG) followed by immunoprecipitation of the PDI fragments. Analysis of the immunoprecipitates revealed that both PDI fragments bound CTA1 under the reducing but not oxidizing condition (Fig. 3.3C, top panel, compare lanes 5 and 6 to lanes 7 and 8). Thus, we conclude PDI*abb'x* and PDI*bb'xa'* interact with CTA1 in a redox-driven manner similar to full-length PDI (Tsai and Rapoport, 2002; Tsai et al., 2001).

Additional determinants of PDI's unfoldase activity

Because a strong PDI-toxin interaction was not sufficient to unfold CTA1, we tested whether the specific linear arrangement of *bb'xa'* and/or identity of the a-type domain (*a'* versus *a*) C-terminal to *bb'x* are additional determinants of PDI's unfoldase activity. Thus, we exchanged the positions of PDI's *a* and *a'* domains, generating the purified PDI*bb'xa* and PDI*a'bb'x* (Fig. 3.4A, lanes 1 and 2), and tested their abilities to unfold

CTA1 using the trypsin-sensitivity assay. Neither PDI*bb'xa* nor PDI*a'bb'x* rendered CTA1 sensitive to tryptic digestion (Fig. 3.4B, compare lanes 3 and 4 to 1 and 2), indicating neither fragment unfolded the toxin. In contrast, co-immunoprecipitation experiments revealed that PDI*bb'xa* bound the toxin with an efficiency similar to PDI*bb'xa'* (Fig. 3.4C, top panel, compare lane 7 to 6). Thus, domain *a* binds CTA1 regardless of its position relative to the *bb'x* domains (Figs. 3.3B and 3.4C), although neither interaction induces the toxin's unfolding (Figs. 3.2B and 3.4B). In contrast, PDI*a'bb'x* bound less CTA1 compared to PDI*bb'xa'* (Fig. 3.4C, top panel, compare lane 8 to 6), indicating domain *a'* must be C-terminal to *bb'x* to efficiently bind and unfold the toxin.

Because the PDI fragments *bb'xa* and *a'bb'x* lack unfoldase activity, we assessed the structural integrity of these purified fragments using limited proteolysis. PDI*bb'xa* was insensitive to proteolysis, similar to PDI*bb'xa'* (Fig. 3.4D, lanes 5-8 compared to lanes 1-4), indicating that they are structurally intact. In contrast, PDI*a'bb'x* was more susceptible to proteolysis than PDI*bb'xa*' or PDI*abb'x* (Fig. 3.4D, compare lanes 9-12 to lanes 1-4 and 13-16); however, the generation of defined proteolytic fragments derived from PDI*a'bb'x* (Fig. 3.4D, lanes 11 and 12, * and **) suggests it is destabilized locally rather than misfolded globally. Thus, we conclude that, in addition to an efficient PDI-toxin interaction, both the specific linear arrangement of *bb'xa'* and the type of *a* domain (*a'* versus *a*) C-terminal to *bb'x* are determinants of PDI's unfoldase activity. We also tested whether the flexibility between the *b'* and *a'* domains (Tian et al., 2008), mediated by the *x* linker (Nguyen et al.), is important for this activity. PDI*bb'a'*, lacking *x*, was unable to unfold CTA1 (data not shown); however, because PDI*bb'a'* was significantly more sensitive to proteolysis than PDI*bb'xa'*, this result is difficult to interpret.

Functional differences between thioredoxin-like domains of PDI and ERp57

We next tested whether the thioredoxin-like domains from ERp57, the closest known PDI homologue (Ferrari and Soling, 1999), can functionally replace PDI's thioredoxin-like domains to generate an unfoldase. ERp57 has the same overall architecture as PDI (Fig. 3.5A). We showed previously that ERp57 is not involved in CTA1 retrotranslocation

(Forster et al., 2006), consistent with its inability to unfold CTA1 *in vitro* (data not shown). In the context of the minimum domains required to unfold CTA1, *bb'xa'*, we tested whether replacing PDI's *bb'* or *a*' domains with the corresponding domains from ERp57 produces an unfoldase. Hence, we generated purified PDI*bb'*-ERp57*xa'* and ERp57*bb'x*-PDI*a*', along with ERp57*bb'xa*' (Fig. 3.5B), and tested their unfoldase activity using the trypsin-sensitivity assay (Fig. 3.5C). PDI*bb'*-ERp57*xa'* unfolded CTA1, whereas ERp57*bb'xa*' and ERp57*bb'x*-PDI*a*' were inactive (Fig. 3.5C, compare lanes 4 and 2 to lanes 5 and 3). (We used the *x* linker from ERp57, rather than from PDI, in the PDI-ERp57 hybrid because a hybrid containing PDI's *x* linker appeared structurally unstable.) ERp57*bb'x*-PDI*a*' displayed a proteolysis pattern similar to ERp57*bb'xa*' and PDI*bb*'-ERp57*xa'* (Fig. 3.5D, compare lanes 9-12 to lanes 1-4 and 5-8), suggesting the inability of ERp57*bb'x*-PDI*a*' to unfold CTA1 is not due to its global misfolding. Addition of ERp57's *a* domain to the active PDI*bb'*-ERp57*xa'* hybrid, generating ERp57*a*-PDI*bb'*-ERp57*xa*' (Fig. 3.5E), rendered the hybrid unable to unfold CTA1 (Fig. 3.5F, compare lane 3 to 4). Furthermore, less CTA1 co-precipitated with ERp57*a*-PDI*bb'*-ERp57*xa*' than with PDI*bb'*-ERp57*xa'* (Fig. 3.5G, top panel, compare lane 4 to 3), indicating ERp57's *a* domain inhibited the unfolding reaction by interfering with the ability of PDI*bb'*-ERp57*xa'* to bind CTA1.

We hypothesized that ERp57's *a* domain disrupts toxin binding because the *a*-*b* junction of ERp57*a*-PDI*bb'*-ERp57*xa*' is more flexible than the corresponding junction of PDI*abb'xa'* enabling ERp57's *a* domain to collapse onto PDI's *bb*' domains. Thus, we subjected ERp57*a*-PDI*bb'*-ERp57*xa*' and PDI*abb'xa'* to limited proteolysis. Discrete fragments derived from ERp57*a*-PDI*bb'*-ERp57*xa*' but not PDI*abb'xa'* appeared (Fig. 3.5H, top panel, compare lane 6 to 3). Importantly, fragment 3 reacted with an anti-PDI but not an anti-His antibody (Fig. 3.5H, compare middle and bottom panels, lane 6), indicating that fragment 3 lost the N-terminal His-tag appended to domain *a*. Because fragment 3 is approximately the same size as PDI*bb'*-ERp57*xa*' (Fig. 3.5B), the simplest explanation is that ERp57's *a* domain was removed by proteolysis. These data imply the *a*-*b* junction of ERp57*a*-PDI*bb'*-ERp57*xa*' is more flexible than the corresponding junction of PDI*abb'xa'*, which might explain why addition of ERp57's *a* domain to

PDI*bb'*-ERp57*xa'* inhibited toxin binding. Thus, we conclude that PDI's *a'* domain but not its *abb'* domains can be partially replaced by the corresponding ERp57 domains to generate an unfoldase.

Functional differences between thioredoxin-like domains of PDI and ERp72

We also tested whether any of the *bb'xa'* domains from the PDI family protein ERp72 can be used to generate an unfoldase. Full-length ERp72 comprises three a-type, two b-type thioredoxin-like domains, an *x* linker, and an acidic extension (*c*) arranged *ca°abb'xa'* (Fig. 3.6A). We purified ERp72*bb'xa*', PDI*bb'x*-ERp72*a'*, and ERp72*bb'x*-PDI*a*' and tested their abilities to unfold CTA1 using the trypsin-sensitivity assay (Fig. 3.6B). ERp72*bb'xa*' was inactive (Fig. 3.6C, compare lane 3 to 2), consistent with our previous report showing that full-length ERp72 stabilizes a folded conformation of the toxin (Forster et al., 2006). PDI*bb'x*-ERp72*a*' was partially able to unfold CTA1 (Fig. 3.6C, compare lane 6 to 5), whereas ERp72*bb'x*-PDI*a*' was inactive (Fig. 3.6C, compare lane 7 to 5). The activity of PDI*bb'x*-ERp72*a'* correlates with its ability to bind CTA1, albeit with slightly reduced efficiency compared to PDI*bb'xa'* (Fig. 3.6D, compare lane 3 to 2). Finally, we assessed the structural integrity of the inactive ERp72*bb'x*-PDI*a*' hybrid and found that it was only slightly more sensitive to proteolysis than ERp72*bb'xa*' or PDI*bb'x*-ERp72*a'* (Fig. 3.6E, compare lanes 5-8 to lanes 1-4 and 9-12), indicating its inactivity is unlikely due to its gross misfolding. Thus, the various PDI-ERp72 and PDI-ERp57 hybrids display a similar trend in their abilities to unfold CTA1 indicating the PDI *bb'x* domains are indispensable for the unfolding reaction, whereas the *a'* domain from other PDI family proteins can be used to generate an unfoldase.

Discussion

This study identifies general structural features of PDI required to unfold CTA1, thus providing insight into the mechanism of its unfoldase activity. Specifically, we found that binding of CTA1 by PDI's linked *bb'xa'* domains is necessary and sufficient to unfold CTA1 efficiently. Moreover, our data indicate a strong PDI-toxin interaction is not sufficient to trigger unfolding; the specific linear arrangement of *bb'xa'* and identity of the a-type domain (*a'* versus *a*) C-terminal to *bb'x* are additional determinants of activity.

We also show that PDI's *bb'* domains are indispensable to the unfolding reaction, whereas the function of its *a'* domain can be substituted partially by domain *a'* from ERp57 or ERp72. However, PDI's *bb'* domains were not sufficient to convert full-length ERp57 into an unfoldase because ERp57's *a* domain inhibited the unfolding reaction.

Consistent with our discovery that PDI*bb'xa'* is necessary and sufficient to unfold CTA1, oxidation of PDI's *a'* domain by Ero1 causes PDI to release the unfolded toxin (Tsai and Rapoport, 2002). Whether PDI*bb'xa'* is sufficient to facilitate retrotranslocation remains to be determined and will reveal whether domains *a* and *c* are required *in vivo*, perhaps to interact with components of the retrotranslocation machinery (Bernardi et al., 2008).

Although PDI*bb'xa'* was sufficient to bind and unfold CTA1 with maximum efficiency, our data show that all four PDI thioredoxin-like domains can interact with the toxin. Interestingly, PDI*bb'xa'* and PDI*abb'x* bound CTA1 with similar efficiencies, but PDI*abb'x* did not unfold the toxin indicating an efficient interaction is not sufficient to trigger unfolding. Because domain *a* was not required to unfold CTA1, it is unclear whether it binds the toxin in the context of full-length PDI. Nevertheless, hydrophobic regions suitable for binding nonnative proteins are present on each PDI thioredoxin-like domain (Kemmink et al., 1996; Tian et al., 2006), and each domain has been shown to contribute to binding substrates (Klappa et al., 1998; Pirneskoski et al., 2001). Moreover, specific hydrophobic residues that mediate substrate interactions have been identified on PDI's *a*, *b'*, and *a'* domains (Koivunen et al., 2005; Pirneskoski et al., 2004). Future studies are required to test whether these same sites are critical for the PDI-toxin interaction, revealing whether differences in the nature of PDI's interactions with its substrates might explain its different activities.

In addition to the requirement for a strong PDI-toxin interaction, we show the specific linear arrangement of *bb'xa'* is required to trigger the toxin's unfolding. Similarly, the arrangement of domains is important for PDI's oxidoreductase functions during protein folding (Kulp et al., 2006). That the *bb'xa'* domains, in this specific arrangement, are required to interact efficiently with CTA1 indicates the binding site on each domain must

be aligned to bind CTA1 concurrently, and this continuous binding site is asymmetric. Thus, we propose a general mechanism for the unfolding reaction: the concurrent binding of the *bb'xa'* domains to particular regions along the CTA1 molecule triggers the toxin's unfolding.

PDI's *a* domain cannot functionally replace its *a'* domain in the unfolding reaction, indicating domain *a'* is intrinsically suited for this activity. This is also true for PDI's function as a P4H subunit (Pirneskoski et al., 2001). Because either a-type domain positioned C-terminal to *bb'x* promoted a stable PDI-toxin interaction, their functional difference is likely due to differences in precisely how they interact with CTA1. Indeed, domain *a* but not *a'* promoted stable toxin binding regardless of its relative position to *bb'x*, implying domain *a'* has a higher binding specificity than domain *a*. The notion that domain *a'* is intrinsically suited for the unfolding reaction is further supported by our finding that PDI's *a'* domain can be substituted partially by the *a'* domain from ERp57 or ERp72. Comparison of the amino acid sequence of PDI's *a'* domain to its *a* domain (~40% identical) and to the ERp57 and ERp72 *a'* domains (each ~50% identical) will help to identify unique features of PDI's *a'* domain that are critical for the unfolding reaction.

Analysis of the unfoldase activity of thioredoxin-like domains from PDI, ERp57, and ERp72 indicates a principle functional difference lies in their *bb'* domains. Indeed, these domains have lower amino acid sequence homology (20-25% identical) than their a-type domains (40-50% identical) and have differences in their binding specificities (Kramer et al., 2001; Maattanen et al., 2006; Oliver et al., 1997; Pirneskoski et al., 2001). Nonetheless, PDI's *bb'* domains were unable to convert full-length ERp57 into an unfoldase, showing their *a* domains also differ functionally. Our data suggest this difference is because the *a-b* junction of ERp57a-PDI*bb'-ERp57xa'* is more flexible than the corresponding junction in PDI*abb'xa'*, enabling ERp57's *a* domain to inhibit toxin binding. Thus, functional differences between PDI and ERp57 might also be due to differences in molecular flexibility (Frickel et al., 2004; Li et al., 2006; Tian et al., 2008). Moreover, these data suggest that although PDI's *a* domain does not contribute directly to the unfolding reaction, it indirectly plays a role by not inhibiting the PDI-toxin

interaction. Thus, we propose that generating an unfoldase from thioredoxin-like domains requires PDI's *bb'(x)* domains followed by an *a'* domain but not preceded by an *a* domain that inhibits toxin binding.

A comparison of the structural requirements for PDI's multiple activities reveals both differences and similarities. Whereas PDI*bb'xa'* is sufficient for maximum unfoldase activity, all four thioredoxin-like domains are required for maximum isomerization of nonnative proteins requiring conformational changes (Darby and Creighton, 1995; Darby et al., 1998) and for full function as a P4H subunit (Pirneskoski et al., 2001). However, similar to the requirements for unfoldase activity, fragments lacking domain *a'* were less efficient at these activities than fragments lacking domain *a*. Therefore, in addition to PDI's *bb'* domains being essential for maximum activity, a trend among PDI's multiple activities is that domain *a'* plays a more critical role than domain *a* (Darby et al., 1998; Pirneskoski et al., 2001), and domain *c* is not required (Koivunen et al., 1999). The differences and similarities highlighted here can be used to design studies to understand in detail how PDI mediates its different activities.

In conclusion, this study identifies key structural requirements for the unfolding reaction suggesting a general mechanism for PDI's unfoldase activity: the concurrent and specific binding of PDI's *bb'xa'* domains to particular regions of CTA1 triggers the toxin's unfolding while domain *a* is neutral. In addition, experiments using PDI, ERp57, and ERp72 indicate that differences in the primary structures of their *abb'* domains account for some of their functional differences. A more detailed comparison of the unfoldase-active to the unfoldase-inactive thioredoxin-like domains of PDI, ERp72, and ERp57 will provide additional clues about the mechanism of PDI's unfoldase activity and greater insight into the molecular basis of their functional differences.

Experimental Methods

Generation of Expression Vectors

cDNA inserts were synthesized by PCR using mouse PDI, human ERp57, or mouse ERp72 cDNA as a template and cloned into vector pQE30 (Qiagen), which encodes an

N-terminal 6xHis-tag. PDI domain boundaries were chosen based on predictions by Pirneskoski *et al.* (Pirneskoski et al., 2004), whereas ERp57 and ERp72 domains were defined based on their sequence homology to PDI. The numbering of each construct refers to the amino acid sequence of the corresponding immature protein. Thus, the full-length PDI construct encodes amino acids D20-L509 corresponding to mature PDI. Construct PDI*abb'xa'* encodes D20-S474; PDI*abb'x* encodes D20-P370; PDI*ab* encodes D20-N243; PDI*bb'a'c* encodes A139-L509; PDI*bb'xa'* encodes A139-S474; PDI*bb'a'* encodes A139-G351 followed by V371-S474; PDI*bb'x* encodes A139-P370; PDI*b'xa'* encodes Q235-S474. Construct PDI*a'bb'x* encodes V371-S474 followed by A139-P370, and PDI*bb'xa* encodes A139-P370 followed by D20-A138. Construct ERp57*bb'xa'* encodes amino acids S136-R482 of ERp57; PDI*bb'*-ERp57x*a'* encodes A139-G351 of PDI followed by N360-R482 of ERp57; ERp57*bb'x*-PDI*a'* encodes S136-P377 of ERp57 followed by V371-S474 of PDI. Construct ERp72*bb'xa'* encodes amino acids K281-T634 of ERp72; PDI*bbx*-ERp72*a'* encodes A139-P370 of PDI followed by V520-T634 of ERp72; ERp72*bb'x*-PDI*a'* encodes K281-P519 of ERp72 followed by V371-S474 of PDI. Construct ERp57*a*-PDI*bb'*-ERp57*xa'* encodes S25-A135 of ERp57 followed by the PDI*bb'*-ERp57*xa'* sequence. The cDNA inserts for PDI*bb'*-ERp57x*a'* and PDI*bbx*-ERp72*a'* were cloned between the Xma1 and Sal1 sites of pQE30. All other cDNA inserts were cloned between the Sph1 and Xma1 sites.

Protein Expression and Purification

The pQE30 constructs were expressed in *E.coli* strain BL21-Pro (Clontech) for 2-4 hrs at 37°C upon induction with isopropylthio-β-galactoside (1 mM, Invitrogen). Cells were lysed by incubation in buffer containing 1% triton X-100, 300 mM KOAc, 250 mM sucrose, 2mM $Mg(OAc)_2$, and 50 mM HEPES at pH 7.5 followed by sonication. Lysates were centrifuged and the resulting supernatant fractions applied to an Ni-nitrilotriacetic acid agarose column (Qiagen) in the presence of Imidazole (20 mM, Sigma) and reduced glutathione (GSH, 3 mM, Sigma). His-tagged proteins were eluted from the column with Imidazole (100, 300, or 500 mM). Eluates containing the purified proteins were dialyzed overnight in physiological buffer (150 mM KOAc, 250 mM sucrose, 2mM $Mg(OAc)_2$, and 50 mM HEPES at pH 7.5) containing GSH (1-3 mM).

Trypsin-Sensitivity Assay to Detect Unfolded CTA1

CTA (50 nM, EMD Biosciences) was incubated with purified PDI or BSA (5.5 μM) in physiological buffer with GSH (3 mM) at 30°C for 30 min. The samples were next incubated with or without trypsin (10 μM, Sigma) at 4°C for 30 min followed by incubation with the trypsin inhibitor tosyl-L-lysyl-chloromethane hydrochloride (TLCK, 10 mg/mL, Sigma) for 10 min at 4°C. Samples were resolved by reducing SDS-PAGE and analyzed by immunoblotting with an anti-CTA antibody generated in the Tsai lab.

Co-immunoprecipitation

CTA (50 nM) was incubated with purified His-tagged proteins (5.5 μM) in physiological buffer containing GSH or GSSG (3 mM) for 30 min at 30°C to stimulate the unfolding reaction. Next, His-tagged proteins were immunoprecipitated using an anti-His antibody (H-15, Santa Cruz Biotechnology) for 1 hr at 4°C. Immune complexes were isolated by incubation with protein A agarose beads (Invitrogen) for 30 min at 4°C and resolved by reducing SDS-PAGE. CTA1 was detected by immunoblotting with our anti-CTA antibody, whereas PDI proteins were detected by Western blotting with an anti-PDI antibody (H-160, Santa Cruz Biotechnology) or by Coomassie staining the gel.

Limited Proteolysis of Recombinant Proteins

Purified recombinant proteins (7 μM) were incubated with the trypsin concentrations indicated in the Fig. for 30 min at 30ºC in physiological buffer containing GSH (3 mM). Proteolysis was inhibited by incubation with TLCK (10 mg/mL) for 10 min at 4ºC. Samples were subjected to reducing SDS-PAGE, and proteins were visualized with Coomassie stain.

Figure 3.1. Recombinant PDI unfolds CTA1 efficiently.
A. Coomassie stain of His-tagged full-length PDI (PDI-FL) purified from bacteria and subjected to SDS-PAGE. B. CTA was incubated with BSA or PDI in the presence of GSH at 30°C followed by incubation with or without trypsin at 4°C. Samples were resolved by reducing SDS-PAGE and analyzed by immunoblotting with an anti-CTA antibody that recognizes CTA1. C. As in B. except CTA was incubated with PDI at 4°C or 30°C before incubation with trypsin at 4°C.

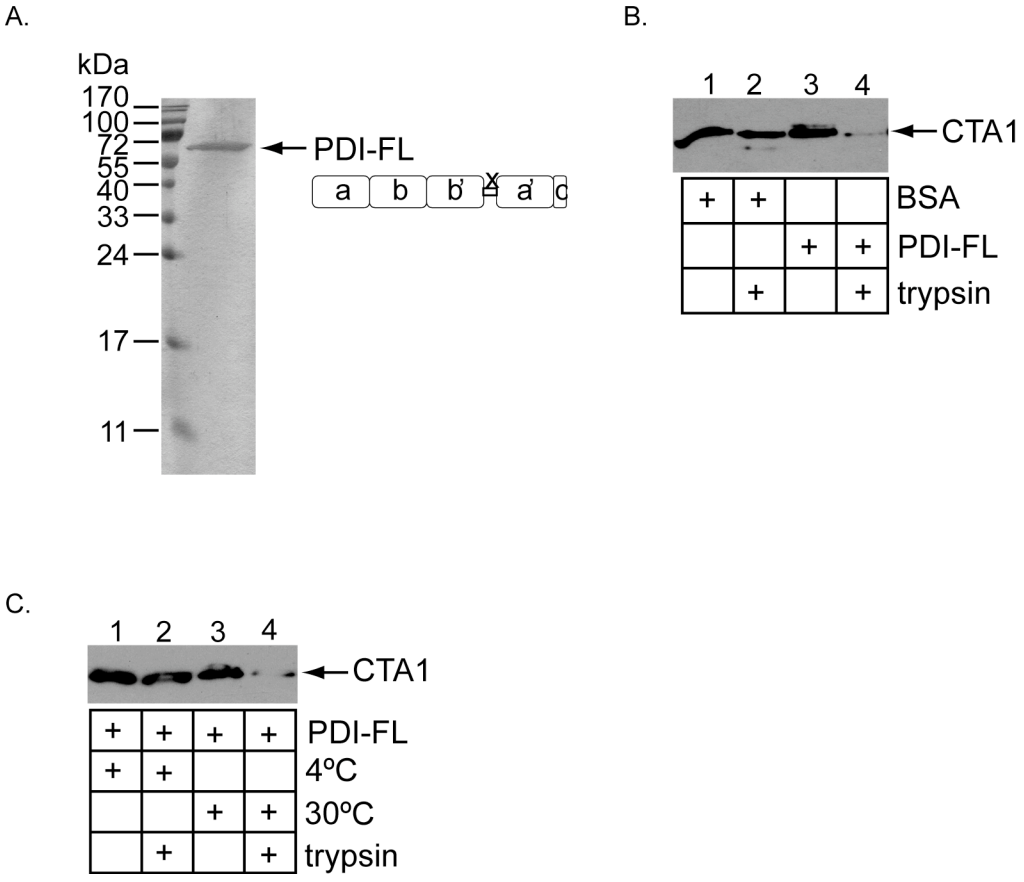

Figure 3.2. PDI's bb'xa' domains form the minimum unit required to unfold CTA1.
A. Coomassie stain of the indicated His-tagged PDI proteins purified from bacteria and subjected to SDS-PAGE. B. CTA was incubated with the indicated proteins in the presence of GSH followed by incubation with trypsin. Samples were analyzed by SDS-PAGE and immunoblotting with an anti-CTA antibody. C. CTA was incubated with PDI*abb'xa'* or an equal molar amount of PDI*ab* and PDI*b'xa'* and analyzed as in B.

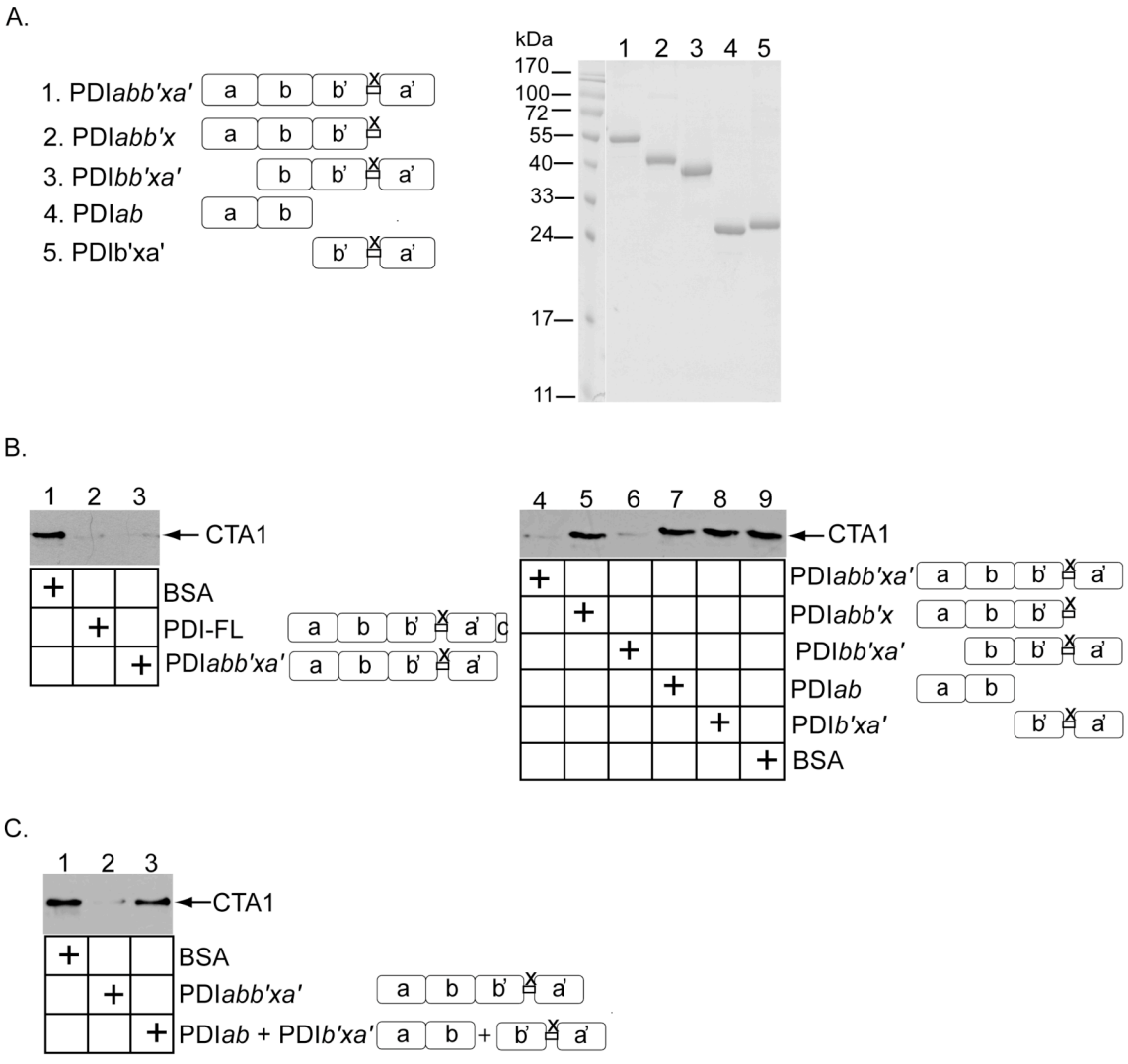

Figure 3.3. A PDI-toxin interaction is necessary but not sufficient to trigger unfolding.
A. CTA was incubated with the indicated proteins in the presence of GSH to stimulate unfolding. PDI-toxin complexes were then isolated by co-immunoprecipitation with an antibody against the His-tag on PDI and resolved by reducing SDS-PAGE. CTA1 was detected by immunoblot analysis using an anti-CTA antibody (top); ERp29 was detected by Coomassie stain (middle) and PDI was detected by immunoblotting with an anti-PDI antibody (bottom). B. As in A except PDI proteins were detected with Coomassie stain only. C. CTA was incubated with the indicated proteins in the presence of GSH or GSSG. Immunoprecipitation and analysis was performed as in A.

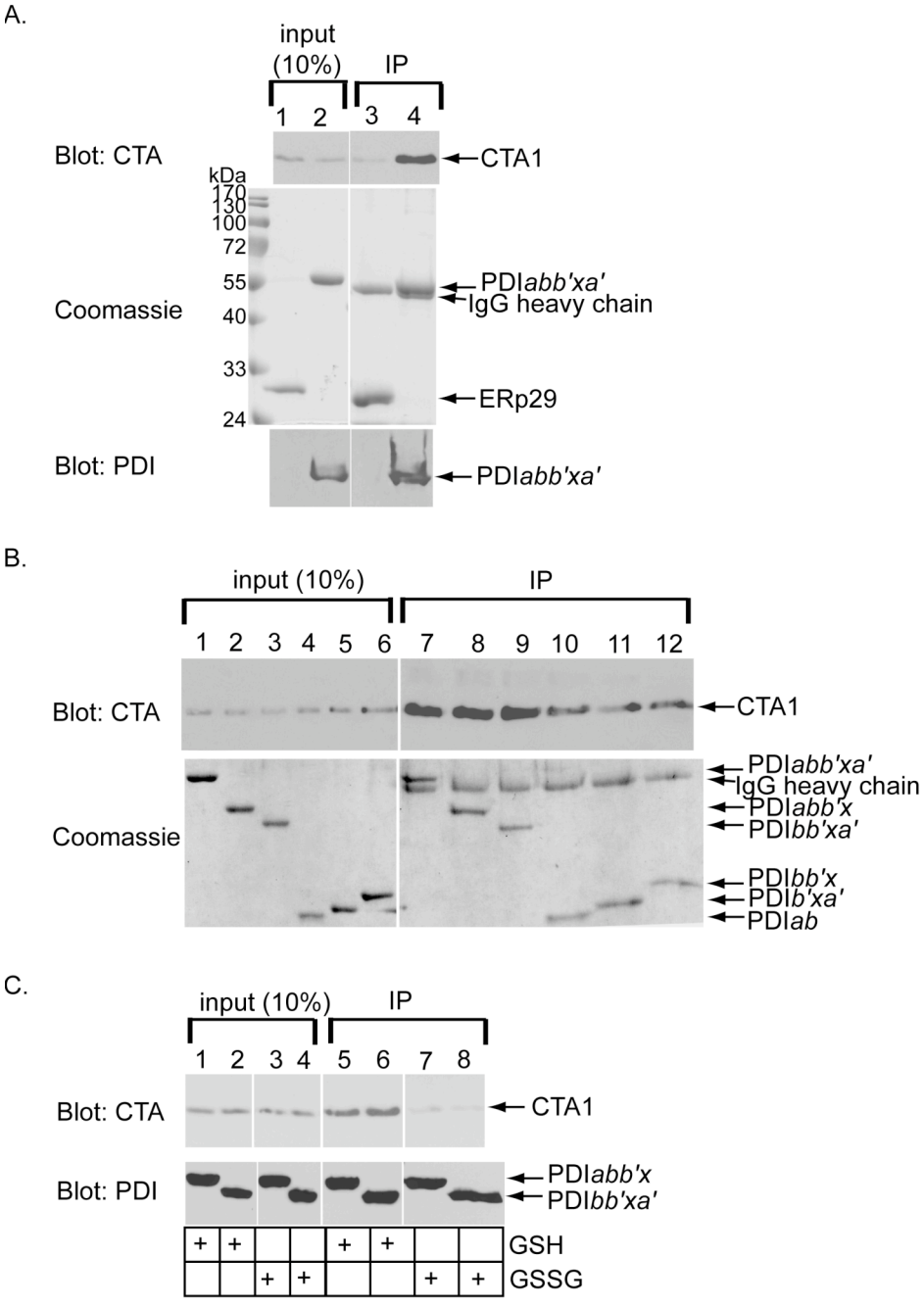

Figure 3.4. The specific linear arrangement and identity of domains are determinants of unfoldase activity. A. Coomassie stain of the indicated His-tagged proteins purified from bacteria and subjected to SDS-PAGE. B. CTA was incubated with the indicated proteins in the presence of GSH followed by incubation with trypsin. CTA1 was detected by SDS-PAGE followed by immunoblotting with an anti-CTA antibody. C. CTA was incubated with the indicated proteins in the presence of GSH to stimulate the unfolding reaction. PDI-toxin complexes were isolated by co-immunoprecipitation with an antibody against the His-tag on PDI and resolved by reducing SDS-PAGE. CTA1 was detected by immunoblot analysis using an anti-CTA antibody (top), and PDI proteins detected by Coomassie stain (bottom). D. Coomassie stain of the indicated proteins subjected to SDS-PAGE after incubation with the indicated amounts of trypsin.

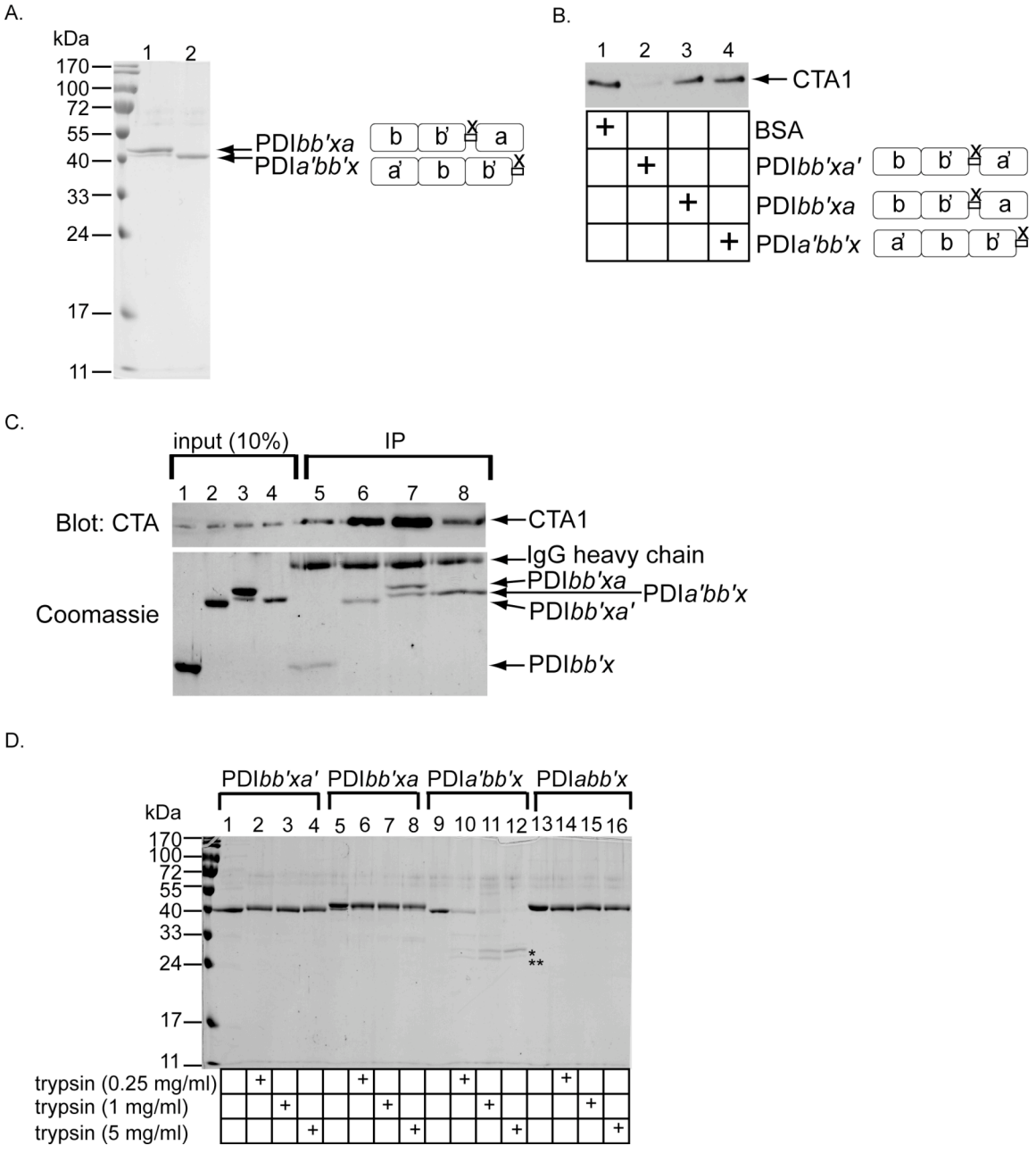

Figure 3.5. Functional differences between thioredoxin-like domains of PDI and ERp57.
A. Diagram of the domain architectures of full-length PDI and ERp57, designated FL for full-length. B. Coomassie stain of the indicated His-tagged proteins purified from bacteria and subjected to SDS-PAGE. C. CTA was incubated with the indicated proteins in the presence of GSH followed by incubation with trypsin. Samples were resolved by SDS-PAGE and immunoblotted with an anti-CTA antibody. D. Coomassie stain of the indicated proteins subjected to SDS-PAGE after incubation with the indicated amounts of trypsin. E. Coomassie stain of ERp57*a*-PDI*bb'*-ERp57*xa'* purified from bacteria and subjected to SDS-PAGE. F. As in C. G. CTA was incubated with the indicated proteins in the presence of GSH. Recombinant proteins were then immunoprecipitated with an anti-His antibody and subjected to reducing SDS-PAGE. Co-precipitated CTA1 was detected by immunoblotting with an anti-CTA antibody (top), and the His-tagged proteins were detected by Coomassie stain (bottom). H. Coomassie stain of the indicated proteins subjected to SDS-PAGE after incubation with the indicated amounts of trypsin.

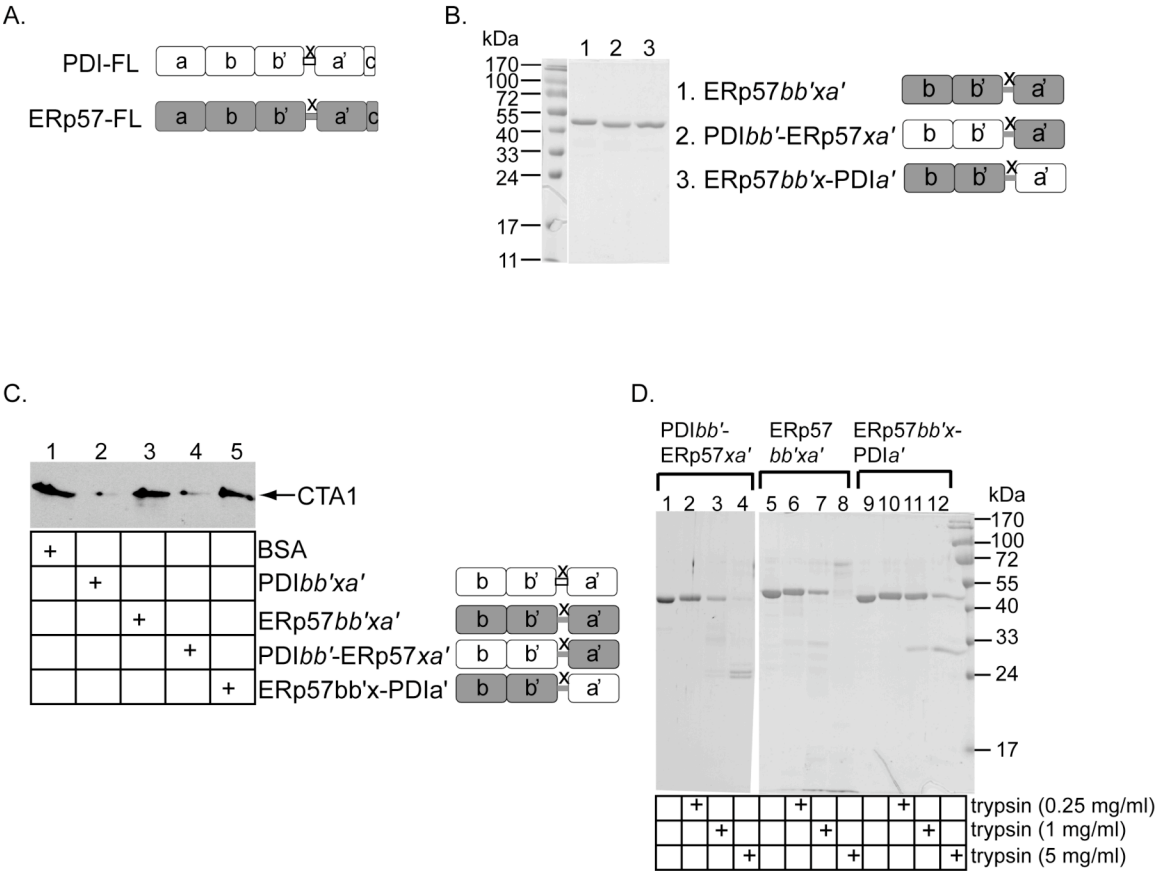

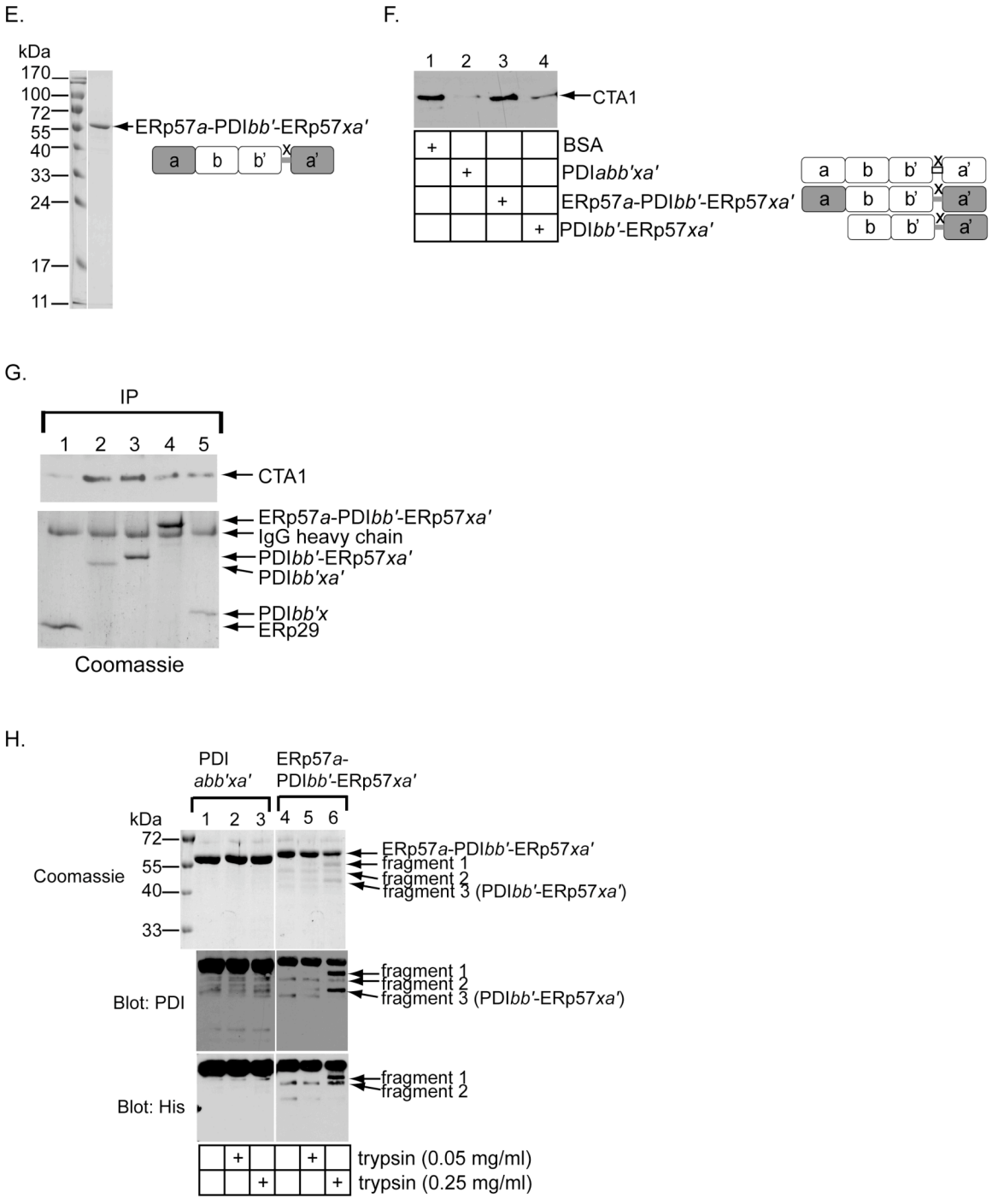
E.
kDa
170
100
72
55
40
33
24
17
11
ERp57a-PDIbb'-ERp57xa'
a
b
b'
x
a'
F.
1 2 3 4
CTA1
BSA
PDIabb'xa'
ERp57a-PDIbb'-ERp57xa'
PDIbb'-ERp57xa'
G.
IP
1 2 3 4 5
CTA1
ERp57a-PDIbb'-ERp57xa'
IgG heavy chain
PDIbb'-ERp57xa'
PDIbb'xa'
PDIbb'x
ERp29
Coomassie
H.
PDI abb'xa'
ERp57a-PDIbb'-ERp57xa'
kDa
1 2 3 4 5 6
72
55
40
33
Coomassie
ERp57a-PDIbb'-ERp57xa'
fragment 1
fragment 2
fragment 3 (PDIbb'-ERp57xa')
Blot: PDI
fragment 1
fragment 2
fragment 3 (PDIbb'-ERp57xa')
Blot: His
fragment 1
fragment 2
trypsin (0.05 mg/ml)
trypsin (0.25 mg/ml)

Figure 3.6. Functional differences between thioredoxin-like domains of PDI and ERp72.
A. Diagram of the domain architectures of full-length PDI and ERp72, designated FL for full-length. B. Coomassie stain of the indicated His-tagged proteins purified from bacteria and subjected to SDS-PAGE. C. CTA was incubated with the indicated proteins in the presence of GSH followed by incubation with trypsin. Samples were resolved by SDS-PAGE and immunoblotted with an anti-CTA antibody. D. CTA was incubated with the indicated proteins in the presence of GSH to stimulate the unfolding reaction. Recombinant proteins were immunoprecipitated with an anti-His antibody and subjected to SDS-PAGE. Co-precipitated CTA1 was detected by immunoblotting with an anti-CTA antibody (top); PDI and the PDI-ERp72 hybrid detected using an anti-PDI antibody (middle); and ERp29 detected with an anti-ER29 antibody (bottom). E. Coomassie stain of the indicated proteins subjected to SDS-PAGE after incubation with the indicated amounts of trypsin.

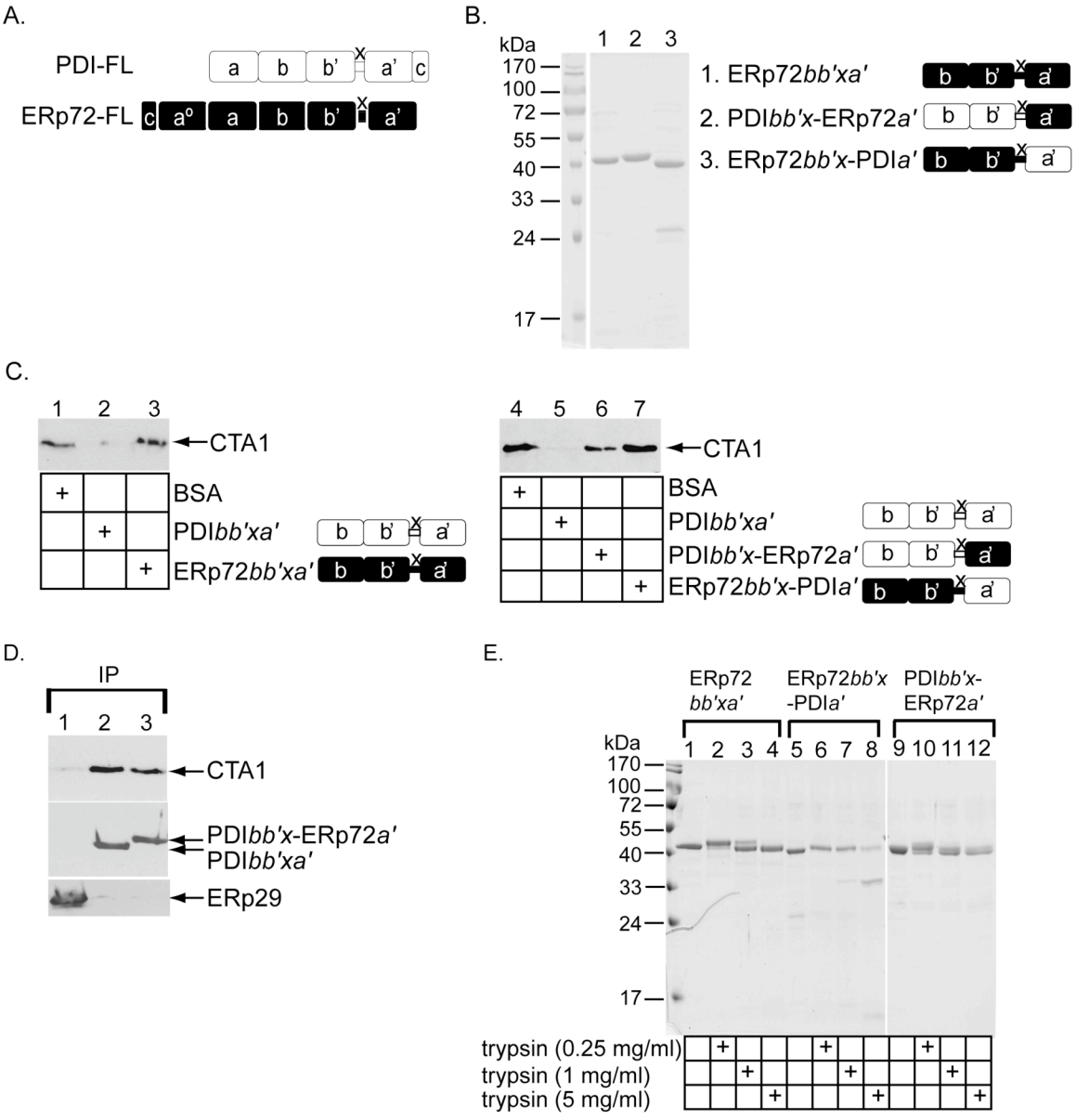

Chapter 4

Conclusion

A detailed understanding of the mammalian ER quality control system is imperative to the development of therapeutics to correct protein misfolding diseases and strategies to defend against pathogenic factors that co-opt this system. In this thesis, we demonstrate that the PDI family proteins PDI and ERp72 are components of the ER quality control machinery and show that they mediate opposing mechanisms (Fig 4.1). Specifically, we found that PDI mediates the retrotranslocation of CTA1 and misfolded proteins (Chapter 2; Forster et al., 2006), consistent with PDI's ability to unfold the toxin *in vitro* (Tsai et al., 2001). In contrast, we found that ERp72 mediates the ER retention of CT and misfolded proteins and stabilizes a folded conformation of the toxin (Chapter 2; Forster et al., 2006). These studies also provide insight into the mechanism of PDI's unfoldase activity and how PDI family proteins mediate diverse activities.

Although PDI was previously implicated in retrotranslocation (Gillece et al., 1999; Molinari et al., 2002; Tsai et al., 2001), the data presented here provide the first evidence that mammalian PDI actively facilitates this process. Moreover, that PDI assists the retrotranslocation of CTA1, a specific misfolded secretory protein (mutant thyroglobulin), and a general population of ERAD substrates indicates that PDI is a general component of the retrotranslocation machinery. In addition, mammalian PDI was shown recently to be the only lumenal ER resident protein required for the retrotranslocation of a misfolded secretory protein using a purified retrotranslocation system (Wahlman et al., 2007). Thus, PDI is a general and critical component of the ER quality control system in mammals.

That PDI unfolds CTA1 *in vitro* (Tsai et al., 2001) and is required for the toxin's efficient

retrotranslocation (Forster et al., 2006) suggests a specific function of PDI is to unfold substrates in preparation for their retrotranslocation. This data provides additional evidence that proteins must be unfolded for retrotranslocation, which has been debated (Beaumelle et al., 1997; Fiebiger et al., 2002; Schlenstedt et al., 1994; Tirosh et al., 2003). Our data combined with previously published data (Tsai et al., 2001) indicate that, in PDI's reduced state, the *bb'xa'* domains bind concurrently to specific regions of the toxin to trigger its unfolding. Oxidation of PDI then causes release of the unfolded toxin (Tsai et al., 2001). Although domain *a* can bind the toxin, it is not required to unfold CTA1 *in vitro*. Therefore, it is unclear whether this domain binds CT in the context of full-length PDI. Whether PDI's *bb'xa'* domains are sufficient to facilitate the retrotranslocation of CTA1 and other proteins remains to be determined.

PDI's unfoldase activity is in contrast to its roles in protein folding. As an oxidoreductase, PDI catalyzes the oxidation and/or isomerization of disulfides of nascent polypeptides to help them fold properly (Goldberger et al., 1964). Independent of redox activity, PDI is a chaperone, binding hydrophobic regions of nonnative polypeptides to prevent their aggregation (Song and Wang, 1995; Wang and Tsou, 1993; Winter et al., 2002). A comparison of the PDI domains required for these diverse activities indicates that PDI interacts with folding and unfolding substrates differently. Thus, the precise nature of the PDI-substrate interaction likely determines the effect that PDI has on the substrate's conformation. Whereas the nature of this interaction is probably determined by a substrate's structural characteristics, future studies are required to understand how PDI chooses between substrates that require folding versus unfolding. That a portion of PDI associates with a membrane component of the retrotranslocation machinery (Bernardi et al., 2008) suggests that PDI's association with partner proteins might regulate which type of substrate PDI interacts with, thereby regulating PDI's activities.

In contrast to PDI's role in retrotranslocation, ERp72 mediates ER retention and perhaps additional attempts at folding, whereas ERp57 does not appear to play a role in either process. Furthermore, we found that only the *a'* domain of ERp57 or ERp72 could partially replace the function of the corresponding PDI domain in the unfolding reaction.

These data indicate that, despite the common tertiary structure of thioredoxin-like domains, these domains are capable of unique activities. This observation is supported by studies showing that PDI family proteins mediate different cellular functions and/or interact with different substrates (reviewed in Appenzeller-Herzog and Ellgaard, 2008). A comparison of the amino acid sequences of the corresponding thioredoxin-like domains of PDI family proteins will help to identify structural features important for their unique functions. Furthermore, how ERp72 refolds or stabilizes the native conformation of CTA1 remains to be determined.

Despite their opposing functions during ER quality control, there is evidence that PDI and ERp72 work co-operatively during protein folding (Satoh et al., 2005). This promotes the idea that retained proteins that fail to fold properly might be passed from ERp72 to PDI for retrotranslocation and degradation. Future studies designed to investigate this possibility might elucidate the transition between the retention of proteins that fail to fold properly and ERAD.

Our data indicate that CTA1 co-opts the ER quality control machinery used by misfolded proteins endogenous to the cell. In addition, CTA1 retrotranslocation was recently shown to rely on Derlin-1, a membrane component of the retrotranslocation machinery (Bernardi et al., 2008). These findings collectively demonstrate that CT can be used to identify general components of the ER quality control system and subsequently elucidate their mechanisms of action. Similar studies using ERAD substrates are confounded by the potential for ER resident proteins that mediate ERAD to also facilitate forward translocation and protein folding. Because CTA1 does not rely on ER factors for its folding and ER import, the toxin is an ideal substrate for specifically studying retrotranslocation and ER retention.

Figure 4.1 PDI family proteins play opposing roles during ER quality control.
See text for discussion.

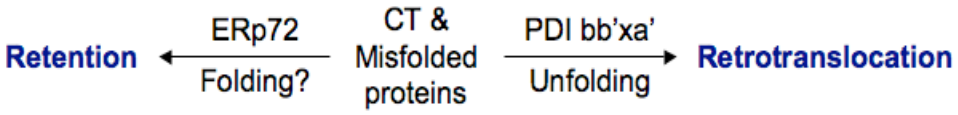

References

Appenzeller-Herzog, C., and Ellgaard, L. (2008). The human PDI family: versatility packed into a single fold. Biochim. Biophys. Acta *1783*, 535-548.

Beaumelle, B., Taupiac, M.P., Lord, J.M., and Roberts, L.M. (1997). Ricin A chain can transport unfolded dihydrofolate reductase into the cytosol. J. Biol. Chem. *272*, 22097-22102.

Bernardi, K.M., Forster, M.L., Lencer, W.I., and Tsai, B. (2008). Derlin-1 facilitates the retro-translocation of cholera toxin. Mol. Biol. Cell *19*, 877-884.

Buck, T.M., Wright, C.M., and Brodsky, J.L. (2007). The activities and function of molecular chaperones in the endoplasmic reticulum. Semin. Cell Dev. Biol. *18*, 751-761.

Cotterill, S.L., Jackson, G.C., Leighton, M.P., Wagener, R., Makitie, O., Cole, W.G., and Briggs, M.D. (2005). Multiple epiphyseal dysplasia mutations in MATN3 cause misfolding of the A-domain and prevent secretion of mutant matrilin-3. Hum. Mutat. *26*, 557-565.

Darby, N.J., and Creighton, T.E. (1995). Functional properties of the individual thioredoxin-like domains of protein disulfide isomerase. Biochemistry *34*, 11725-11735.

Darby, N.J., Kemmink, J., and Creighton, T.E. (1996). Identifying and characterizing a structural domain of protein disulfide isomerase. Biochemistry *35*, 10517-10528.

Darby, N.J., Penka, E., and Vincentelli, R. (1998). The multi-domain structure of protein disulfide isomerase is essential for high catalytic efficiency. J. Mol. Biol. *276*, 239-247.

Darby, N.J., van Straaten, M., Penka, E., Vincentelli, R., and Kemmink, J. (1999). Identifying and characterizing a second structural domain of protein disulfide isomerase. FEBS Lett. *448*, 167-172.

Edman, J.C., Ellis, L., Blacher, R.W., Roth, R.A., and Rutter, W.J. (1985). Sequence of protein disulphide isomerase and implications of its relationship to thioredoxin. Nature *317*, 267-270.

Eilers, M., and Schatz, G. (1986). Binding of a specific ligand inhibits import of a purified precursor protein into mitochondria. Nature *322*, 228-232.

Ellgaard, L., and Helenius, A. (2003). Quality control in the endoplasmic reticulum. Nat. Rev. Mol. Cell Biol. *4*, 181-191.

Ellgaard, L. and Ruddock, L. (2005). The human protein disulfide isomerase family: substrate interactions and functional properties. EMBO Rep. *6*, 28-32.

Ferrari, D.M., and Soling, H.D. (1999). The protein disulphide-isomerase family: unravelling a string of folds. Biochem. J. *339 (Pt 1)*, 1-10.

Fiebiger, E., Story, C., Ploegh, H.L., and Tortorella, D. (2002). Visualization of the ER-to-cytosol dislocation reaction of a type I membrane protein. EMBO J. *21*, 1041-1053.

Forster, M.L., Mahn, J.J., and Tsai, B. (2008). Generating an nfoldase from thioredoxin-like domains.

Forster, M.L., Sivick, K., Park, Y.N., Arvan, P., Lencer, W.I., and Tsai, B. (2006). Protein disulfide isomerase-like proteins play opposing roles during retrotranslocation. J. Cell Biol. *173*, 853-859.

Frickel, E.M., Frei, P., Bouvier, M., Stafford, W.F., Helenius, A., Glockshuber, R., and Ellgaard, L. (2004). ERp57 is a multifunctional thiol-disulfide oxidoreductase. J. Biol. Chem. *279*, 18277-18287.

Fujinaga, Y., Wolf, A.A., Rodighiero, C., Wheeler, H., Tsai, B., Allen, L., Jobling, M.G., Rapoport, T., Holmes, R.K., and Lencer, W.I. (2003). Gangliosides that associate with lipid rafts mediate transport of cholera and related toxins from the plasma membrane to endoplasmic reticulm. Mol. Biol. Cell *14*, 4783-4793.

Gilbert, J., Ou, W., Silver, J., and Benjamin, T. (2006). Downregulation of protein disulfide isomerase inhibits infection by the mouse polyomavirus. J. Virol. *80*, 10868-10870.

Gillece, P., Luz, J.M., Lennarz, W.J., de La Cruz, F.J., and Romisch, K. (1999). Export of a cysteine-free misfolded secretory protein from the endoplasmic reticulum for degradation requires interaction with protein disulfide isomerase. J. Cell Biol. *147*, 1443-1456.

Goldberg, A.L. (2003). Protein degradation and protection against misfolded or damaged proteins. Nature *426*, 895-899.

Goldberger, R.F., Epstein, C.J., and Anfinsen, C.B. (1964). Purification and Properties of a Microsomal Enzyme System Catalyzing the Reactivation of Reduced Ribonuclease and Lysozyme. J. Biol. Chem. *239*, 1406-1410.

Hazes, B., and Read, R.J. (1997). Accumulating evidence suggests that several AB-toxins subvert the endoplasmic reticulum-associated protein degradation pathway to enter target

cells. Biochemistry *36*, 11051-11054.

Karin, M., and Ben-Neriah, Y. (2000). Phosphorylation meets ubiquitination: the control of NF-[kappa]B activity. Annu. Rev. Immunol. *18*, 621-663.

Kemmink, J., Darby, N.J., Dijkstra, K., Nilges, M., and Creighton, T.E. (1996). Structure determination of the N-terminal thioredoxin-like domain of protein disulfide isomerase using multidimensional heteronuclear 13C/15N NMR spectroscopy. Biochemistry *35*, 7684-7691.

Kemmink, J., Darby, N.J., Dijkstra, K., Nilges, M., and Creighton, T.E. (1997). The folding catalyst protein disulfide isomerase is constructed of active and inactive thioredoxin modules. Curr. Biol. *7*, 239-245.

Klappa, P., Ruddock, L.W., Darby, N.J., and Freedman, R.B. (1998). The b' domain provides the principal peptide-binding site of protein disulfide isomerase but all domains contribute to binding of misfolded proteins. EMBO J. *17*, 927-935.

Koivunen, P., Helaakoski, T., Annunen, P., Veijola, J., Raisanen, S., Pihlajaniemi, T., and Kivirikko, K.I. (1996). ERp60 does not substitute for protein disulphide isomerase as the beta-subunit of prolyl 4-hydroxylase. Biochem. J. *316 (Pt 2)*, 599-605.

Koivunen, P., Pirneskoski, A., Karvonen, P., Ljung, J., Helaakoski, T., Notbohm, H., and Kivirikko, K.I. (1999). The acidic C-terminal domain of protein disulfide isomerase is not critical for the enzyme subunit function or for the chaperone or disulfide isomerase activities of the polypeptide. EMBO J. *18*, 65-74.

Koivunen, P., Salo, K.E., Myllyharju, J., and Ruddock, L.W. (2005). Three binding sites in protein-disulfide isomerase cooperate in collagen prolyl 4-hydroxylase tetramer assembly. J. Biol. Chem. *280*, 5227-5235.

Kramer, B., Ferrari, D.M., Klappa, P., Pohlmann, N., and Soling, H.D. (2001). Functional roles and efficiencies of the thioredoxin boxes of calcium-binding proteins 1 and 2 in protein folding. Biochem. J. *357*, 83-95.

Kulp, M.S., Frickel, E.M., Ellgaard, L., and Weissman, J.S. (2006). Domain architecture of protein-disulfide isomerase facilitates its dual role as an oxidase and an isomerase in Ero1p-mediated disulfide formation. J. Biol. Chem. *281*, 876-884.

Lamberg, A., Jauhiainen, M., Metso, J., Ehnholm, C., Shoulders, C., Scott, J., Pihlajaniemi, T., and Kivirikko, K.I. (1996). The role of protein disulphide isomerase in the microsomal triacylglycerol transfer protein does not reside in its isomerase activity. Biochem. J. *315 (Pt 2)*, 533-536.

Le Gall, S., Neuhof, A., and Rapoport, T. (2004). The endoplasmic reticulum membrane is permeable to small molecules. Mol. Biol. Cell *15*, 447-455.

Lencer, W.I., Constable, C., Moe, S., Rufo, P.A., Wolf, A., Jobling, M.G., Ruston, S.P., Madara, J.L., Holmes, R.K., and Hirst, T.R. (1997). Proteolytic activation of cholera toxin and Escherichia coli labile toxin by entry into host epithelial cells. Signal transduction by a protease-resistant toxin variant. J. Biol. Chem. *272*, 15562-15568.

Lencer, W.I. (2001). Microbes and microbial Toxins: paradigms for microbial-mucosal toxins. V. Cholera: invasion of the intestinal epithelial barrier by a stably folded protein toxin. Am. J. Physiol. Gastrointest. Liver Physiol. *280*, G781-786.

Lencer, W.I., and Tsai, B. (2003). The intracellular voyage of cholera toxin: going retro. Trends Biochem. Sci. *28*, 639-645.

Li, S.J., Hong, X.G., Shi, Y.Y., Li, H., and Wang, C.C. (2006). Annular arrangement and collaborative actions of four domains of protein-disulfide isomerase: a small angle X-ray scattering study in solution. J. Biol. Chem. *281*, 6581-6588.

Maattanen, P., Kozlov, G., Gehring, K., and Thomas, D.Y. (2006). ERp57 and PDI: multifunctional protein disulfide isomerases with similar domain architectures but differing substrate-partner associations. Biochem. Cell Biol. *84*, 881-889.

Majoul, I.V., Bastiaens, P.I., and Soling, H.D. (1996). Transport of an external Lys-Asp-Glu-Leu (KDEL) protein from the plasma membrane to the endoplasmic reticulum: studies with cholera toxin in Vero cells. J. Cell Biol. *133*, 777-789.

McClellan, A.J., Scott, M.D., and Frydman, J. (2005). Folding and quality control of the VHL tumor suppressor proceed through distinct chaperone pathways. Cell *121*, 739-748.

Mekalanos, J.J., Collier, R.J., and Romig, W.R. (1979). Enzymic activity of cholera toxin. II. Relationships to proteolytic processing, disulfide bond reduction, and subunit composition. J. Biol. Chem. *254*, 5855-5861.

Molinari, M., Galli, C., Piccaluga, V., Pieren, M., and Paganetti, P. (2002). Sequential assistance of molecular chaperones and transient formation of covalent complexes during protein degradation from the ER. J. Cell Biol. *158*, 247-257.

Nakatsukasa, K., and Brodsky, J.L. (2008). The recognition and retrotranslocation of misfolded proteins from the endoplasmic reticulum. Traffic *9*, 861-870.

Nguyen, V.D., Wallis, K., Howard, M.J., Haapalainen, A.M., Salo, K.E., Saaranen, M.J., Sidhu, A., Wierenga, R.K., Freedman, R.B., Ruddock, L.W., and Williamson, R.A. (2008). Alternative conformations of the x region of human protein disulphide-isomerase modulate exposure of the substrate binding b' domain. J. Mol. Biol. *383*, 1144-1155.

Ni, M., and Lee, A.S. (2007). ER chaperones in mammalian development and human diseases. FEBS Lett. *581*, 3641-3651.

Oliver, J.D., van der Wal, F.J., Bulleid, N.J., and High, S. (1997). Interaction of the thiol-dependent reductase ERp57 with nascent glycoproteins. Science *275*, 86-88.

Papp, E., Száraz, P., Korcsmáros, T., and Csermely, P. (2006). Changes of endoplasmic reticulum chaperone complexes, redox state, and impaired protein disulfide reductase activity in misfolding alpha1-antitrypsin transgenic mice. FASEB J. *20*, 1018-1020.

Park, B., Lee, S., Kim, E., Cho, K., Riddell, S.R., Cho, S., and Ahn, K. (2006). Redox regulation facilitates optimal peptide selection by MHC class I during antigen processing. Cell *127*, 369-382.

Pihlajaniemi, T., Helaakoski, T., Tasanen, K., Myllyla, R., Huhtala, M.L., Koivu, J., and Kivirikko, K.I. (1987). Molecular cloning of the beta-subunit of human prolyl 4-hydroxylase. This subunit and protein disulphide isomerase are products of the same gene. EMBO J. *6*, 643-649.

Pirneskoski, A., Klappa, P., Lobell, M., Williamson, R.A., Byrne, L., Alanen, H.I., Salo, K.E., Kivirikko, K.I., Freedman, R.B., and Ruddock, L.W. (2004). Molecular characterization of the principal substrate binding site of the ubiquitous folding catalyst protein disulfide isomerase. J. Biol. Chem. *279*, 10374-10381.

Pirneskoski, A., Ruddock, L.W., Klappa, P., Freedman, R.B., Kivirikko, K.I., and Koivunen, P. (2001). Domains b' and a' of protein disulfide isomerase fulfill the minimum requirement for function as a subunit of prolyl 4-hydroxylase. The N-terminal domains a and b enhances this function and can be substituted in part by those of ERp57. J. Biol. Chem. *276*, 11287-11293.

Rodighiero, C., Tsai, B., Rapoport, T.A., and Lencer, W.I. (2002). Role of ubiquitination in retro-translocation of cholera toxin and escape of cytosolic degradation. EMBO Rep. *3*, 1222-1227.

Salvador, N., Aguado, C., Horst, M., and Knecht, E. (2000). Import of a cytosolic protein into lysosomes by chaperone-mediated autophagy depends on its folding state. J. Biol. Chem. *275*, 27447-27456.

Satoh, M., Shimada, A., Kashiwai, A., Saga, S., and Hosokawa, M. (2005). Differential cooperative enzymatic activities of protein disulfide isomerase family in protein folding. Cell Stress Chaperones *10*, 211-220.

Schelhaas, M., Malmstrom, J., Pelkmans, L., Haugstetter, J., Ellgaard, L., Grunewald, K., and Helenius, A. (2007). Simian Virus 40 depends on ER protein folding and quality control factors for entry into host cells. Cell *131*, 516-529.

Schlenstedt, G., Zimmermann, M., and Zimmermann, R. (1994). A stably folded presecretory protein associates with and upon unfolding translocates across the membrane of mammalian microsomes. FEBS Lett. *340*, 139-144.

Schnell, D.J., and Hebert, D.N. (2003). Protein translocons: multifunctional mediators of protein translocation across membranes. Cell *112*, 491-505.

Schroder, M., and Kaufman, R.J. (2005). ER stress and the unfolded protein response. Mutat. Res. *569*, 29-63.

Sears, C.L., and Kaper, J.B. (1996). Enteric bacterial toxins: mechanisms of action and linkage to intestinal secretion. Microbiol. Mol. Biol. Rev. *60*, 167-215.

Song, J.L., and Wang, C.C. (1995). Chaperone-like activity of protein disulfide-isomerase in the refolding of rhodanese. Eur. J. Biochem. *231*, 312-316.

Tian, G., Kober, F.X., Lewandrowski, U., Sickmann, A., Lennarz, W.J., and Schindelin, H. (2008). The catalytic activity of protein disulfide isomerase requires a conformationally flexible molecule. J. Biol. Chem.

Tian, G., Xiang, S., Noiva, R., Lennarz, W.J., and Schindelin, H. (2006). The crystal structure of yeast protein disulfide isomerase suggests cooperativity between its active sites. Cell *124*, 61-73.

Tirosh, B., Furman, M.H., Tortorella, D., and Ploegh, H.L. (2003). Protein unfolding is not a prerequisite for endoplasmic reticulum-to-cytosol dislocation. J. Biol. Chem. *278*, 6664-6672.

Tokunaga, F., Brostrom, C., Koide, T., and Arvan, P. (2000). Endoplasmic reticulum (ER)-associated degradation of misfolded N-linked glycoproteins is suppressed upon inhibition of ER mannosidase I. J. Biol. Chem. *275*, 40757-40764.

Tsai, B., and Rapoport, T.A. (2002). Unfolded cholera toxin is transferred to the ER membrane and released from protein disulfide isomerase upon oxidation by Ero1. J. Cell Biol. *159*, 207-216.

Tsai, B., Rodighiero, C., Lencer, W.I., and Rapoport, T.A. (2001). Protein disulfide isomerase acts as a redox-dependent chaperone to unfold cholera toxin. Cell *104*, 937-948.

Tsai, B., Ye, Y., and Rapoport, T.A. (2002). Retro-translocation of proteins from the endoplasmic reticulum into the cytosol. Nat. Rev. Mol. Cell Biol. *3*, 246-255.

Vuori, K., Pihlajaniemi, T., Marttila, M., and Kivirikko, K.I. (1992a). Characterization of the human prolyl 4-hydroxylase tetramer and its multifunctional protein disulfide-isomerase subunit synthesized in a baculovirus expression system. Proc. Natl. Acad. Sci. U. S. A. *89*, 7467-7470.

Vuori, K., Pihlajaniemi, T., Myllyla, R., and Kivirikko, K.I. (1992b). Site-directed

mutagenesis of human protein disulphide isomerase: effect on the assembly, activity and endoplasmic reticulum retention of human prolyl 4-hydroxylase in Spodoptera frugiperda insect cells. EMBO J. *11*, 4213-4217.

Wahlman, J., DeMartino, G.N., Skach, W.R., Bulleid, N.J., Brodsky, J.L., and Johnson, A.E. (2007). Real-time fluorescence detection of ERAD substrate retrotranslocation in a mammalian in vitro system. Cell *129*, 943-955.

Wang, C.C., and Tsou, C.L. (1993). Protein disulfide isomerase is both an enzyme and a chaperone. FASEB J. *7*, 1515-1517.

Wetterau, J.R., Combs, K.A., McLean, L.R., Spinner, S.N., and Aggerbeck, L.P. (1991). Protein disulfide isomerase appears necessary to maintain the catalytically active structure of the microsomal triglyceride transfer protein. Biochemistry *30*, 9728-9735.

Wetterau, J.R., Combs, K.A., Spinner, S.N., and Joiner, B.J. (1990). Protein disulfide isomerase is a component of the microsomal triglyceride transfer protein complex. J. Biol. Chem. *265*, 9800-9807.

Wilkinson, B., and Gilbert, H.F. (2004). Protein disulfide isomerase. Biochim. Biophys. Acta *1699*, 35-44.

Winter, J., Klappa, P., Freedman, R.B., Lilie, H., and Rudolph, R. (2002). Catalytic activity and chaperone function of human protein-disulfide isomerase are required for the efficient refolding of proinsulin. J. Biol. Chem. *277*, 310-317.

Zhang, R.G., Scott, D.L., Westbrook, M.L., Nance, S., Spangler, B.D., Shipley, G.G., and Westbrook, E.M. (1995). The three-dimensional crystal structure of cholera toxin. J. Mol. Biol. *251*, 563-573.

Zhang, Y., Baig, E., and Williams, D.B. (2006). Functions of ERp57 in the folding and assembly of major histocompatibility complex class I molecules. J. Biol. Chem. *281*, 14622-14631.